ITA/AITES Accredited Material

Seismic design and analysis of underground structures

Youssef M.A. Hashash[a,*], Jeffrey J. Hook[a], Birger Schmidt[b],
John I-Chiang Yao[a]

[a]*Department of Civil and Environmental Engineering, University of Illinois at Urbana-Champaign, 205 N. Mathews Avenue, MC-250,
Urbana, IL 61801, USA*
[b]*Parsons Brinckerhoff, San Francisco, CA, USA*

Abstract

Underground facilities are an integral part of the infrastructure of modern society and are used for a wide range of applications, including subways and railways, highways, material storage, and sewage and water transport. Underground facilities built in areas subject to earthquake activity must withstand both seismic and static loading. Historically, underground facilities have experienced a lower rate of damage than surface structures. Nevertheless, some underground structures have experienced significant damage in recent large earthquakes, including the 1995 Kobe, Japan earthquake, the 1999 Chi-Chi, Taiwan earthquake and the 1999 Kocaeli, Turkey earthquake. This report presents a summary of the current state of seismic analysis and design for underground structures. This report describes approaches used by engineers in quantifying the seismic effect on an underground structure. Deterministic and probabilistic seismic hazard analysis approaches are reviewed. The development of appropriate ground motion parameters, including peak accelerations and velocities, target response spectra, and ground motion time histories, is briefly described. In general, seismic design loads for underground structures are characterized in terms of the deformations and strains imposed on the structure by the surrounding ground, often due to the interaction between the two. In contrast, surface structures are designed for the inertial forces caused by ground accelerations. The simplest approach is to ignore the interaction of the underground structure with the surrounding ground. The free-field ground deformations due to a seismic event are estimated, and the underground structure is designed to accommodate these deformations. This approach is satisfactory when low levels of shaking are anticipated or the underground facility is in a stiff medium such as rock. Other approaches that account for the interaction between the structural supports and the surrounding ground are then described. In the pseudo-static analysis approach, the ground deformations are imposed as a static load and the soil-structure interaction does not include dynamic or wave propagation effects. In the dynamic analysis approach, a dynamic soil structure interaction is conducted using numerical analysis tools such as finite element or finite difference methods. The report discusses special design issues, including the design of tunnel segment joints and joints between tunnels and portal structures. Examples of seismic design used for underground structures are included in an appendix at the end of the report. © 2001 Elsevier Science Ltd. All rights reserved.

Keywords: Seismic design; Seismic analysis; Underground structures; Tunnels; Subways; Earthquake design

* Corresponding author. Tel.: +1-217-333-6986; fax: +1-217-265-8041.
E-mail address: hashash@uiuc.edu (Y.M.A. Hashash).

Preface

This paper was developed as part of the activities of the *International Tunnelling Association (ITA) Working Group No 2*: Research. The paper provides a state-of-the-art review of the design and analysis of tunnels subject to earthquake shaking with particular focus on practice in the United States of America. The Authors wish to acknowledge the important contribution of Working Group 2 members including Mr. Yann Leblais, Animateur, Yoshihiro Hiro Takano, Vice-Animateur, Barry New, Member, Henk J.C. Oud and Andres Assis, Tutor and Former Tutor, respectively, as well as the ITA Executive Council for their review and approval of this document.

1. Introduction

Underground structures have features that make their seismic behavior distinct from most surface structures, most notably (1) their complete enclosure in soil or rock, and (2) their significant length (i.e. tunnels). The design of underground facilities to withstand seismic loading thus, has aspects that are very different from the seismic design of surface structures.

This report focuses on relatively large underground facilities commonly used in urban areas. This includes large-diameter tunnels, cut-and-cover structures and portal structures (Fig. 1). This report does not discuss pipelines or sewer lines, nor does it specifically discuss issues related to deep chambers such as hydropower plants, nuclear waste repositories, mine chambers, and protective structures, though many of the design methods and analyses described are applicable to the design of these deep chambers.

Large-diameter tunnels are linear underground structures in which the length is much larger than the cross-sectional dimension. These structures can be grouped into three broad categories, each having distinct design features and construction methods: (1) bored or mined tunnels; (2) cut-and-cover tunnels; and (3) immersed tube tunnels (Power et al., 1996). These tunnels are commonly used for metro structures, highway tunnels, and large water and sewage transportation ducts.

Bored or mined tunnels are unique because they are constructed without significantly affecting the soil or rock above the excavation. Tunnels excavated using tunnel-boring machines (TBMs) are usually circular; other tunnels maybe rectangular or horseshoe in shape. Situations where boring or mining may be preferable to cut-and-cover excavation include (1) significant excavation depths, and (2) the existence of overlying structures.
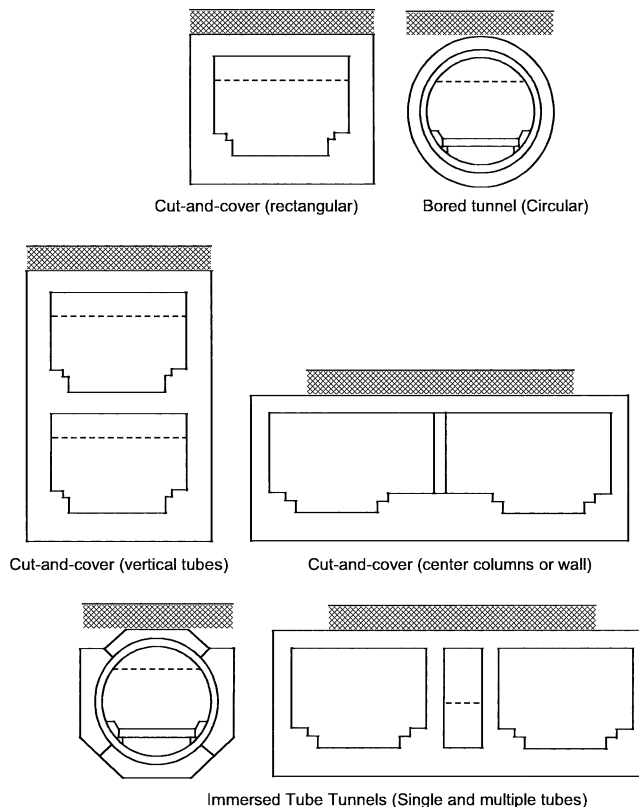

Fig. 1. Cross sections of tunnels (after Power et al., 1996).

Cut-and-cover structures are those in which an open excavation is made, the structure is constructed, and fill is placed over the finished structure. This method is typically used for tunnels with rectangular cross-sections and only for relatively shallow tunnels (< 15 m of overburden). Examples of these structures include subway stations, portal structures and highway tunnels.

Immersed tube tunnels are sometimes employed to traverse a body of water. This method involves constructing sections of the structure in a dry dock, then moving these sections, sinking them into position and ballasting or anchoring the tubes in place.

This report is a synthesis of the current state of knowledge in the area of seismic design and analysis for underground structures. The report updates the work prepared by St. John and Zahrah (1987), which appeared in *Tunneling Underground Space Technol*. The report focuses on methods of analysis of underground structures subjected to seismic motion due to earthquake activity, and provides examples of performance and damage to underground structures during recent major earthquakes. The report describes the overall philosophy used in the design of underground structures, and introduces basic concepts of seismic hazard analysis and methods used in developing design earthquake motion parameters.

The report describes how ground deformations are estimated and how they are transmitted to an under-

ground structure, presenting methods used in the computation of strains, forces and moment in the structure. The report provides examples of the application of these methods for underground structures in Los Angeles, Boston, and the San Francisco Bay Area.

This report does not cover issues related to static design, although static design provisions for underground structures often provide sufficient seismic resistance under low levels of ground shaking. The report does not discuss structural design details and reinforcement requirements in concrete or steel linings for underground structures. The report briefly describes issues related to seismic design associated with ground failure such as liquefaction, slope stability and fault crossings, but does not provide a thorough treatment of these subjects. The reader is encouraged to review other literature on these topics to ensure that relevant design issues are adequately addressed.

2. Performance of underground facilities during seismic events

Several studies have documented earthquake damage to underground facilities. ASCE (1974) describes the damage in the Los Angeles area as a result of the 1971 San Fernando Earthquake. JSCE (1988) describes the performance of several underground structures, including an immersed tube tunnel during shaking in Japan. Duke and Leeds (1959), Stevens (1977), Dowding and Rozen (1978), Owen and Scholl (1981), Sharma and Judd (1991), Power et al. (1998) and Kaneshiro et al. (2000), all present summaries of case histories of damage to underground facilities. Owen and Scholl (1981) have updated Dowding and Rozen's work with 127 case histories. Sharma and Judd (1991) generated an extensive database of seismic damage to underground structures using 192 case histories. Power et al. (1998) provide a further update with 217 case histories. The following general observations can be made regarding the seismic performance of underground structures:

1. Underground structures suffer appreciably less damage than surface structures.
2. Reported damage decreases with increasing overburden depth. Deep tunnels seem to be safer and less vulnerable to earthquake shaking than are shallow tunnels.
3. Underground facilities constructed in soils can be expected to suffer more damage compared to openings constructed in competent rock.
4. Lined and grouted tunnels are safer than unlined tunnels in rock. Shaking damage can be reduced by stabilizing the ground around the tunnel and

by improving the contact between the lining and the surrounding ground through grouting.
5. Tunnels are more stable under a symmetric load, which improves ground-lining interaction. Improving the tunnel lining by placing thicker and stiffer sections without stabilizing surrounding poor ground may result in excess seismic forces in the lining. Backfilling with non-cyclically mobile material and rock-stabilizing measures may improve the safety and stability of shallow tunnels.
6. Damage may be related to peak ground acceleration and velocity based on the magnitude and epicentral distance of the affected earthquake.
7. Duration of strong-motion shaking during earthquakes is of utmost importance because it may cause fatigue failure and therefore, large deformations.
8. High frequency motions may explain the local spalling of rock or concrete along planes of weakness. These frequencies, which rapidly attenuate with distance, may be expected mainly at small distances from the causative fault.
9. Ground motion may be amplified upon incidence with a tunnel if wavelengths are between one and four times the tunnel diameter.
10. Damage at and near tunnel portals may be significant due to slope instability.

The following is a brief discussion of recent case histories of seismic performance of underground structures.

2.1. Underground structures in the United States

2.1.1. Bay Area rapid transit (BART) system, San Francisco, CA, USA

The BART system was one of the first underground facilities to be designed with considerations for seismic loading (Kuesel, 1969). On the San Francisco side, the system consists of underground stations and tunnels in fill and soft Bay Mud deposits, and it is connected to Oakland via the transbay-immersed tube tunnel.

During the 1989 Loma Prieta Earthquake, the BART facilities sustained no damage and, in fact, operated on a 24-h basis after the earthquake. This is primarily because the system was designed under stringent seismic design considerations. Special seismic joints (Bickel and Tanner, 1982) were designed to accommodate differential movements at ventilation buildings. The system had been designed to support earth and water loads while maintaining watertight connections and not exceeding allowable differential movements. No damage was observed at these flexible joints, though it is not exactly known how far the joints moved during the earthquake (PB, 1991).
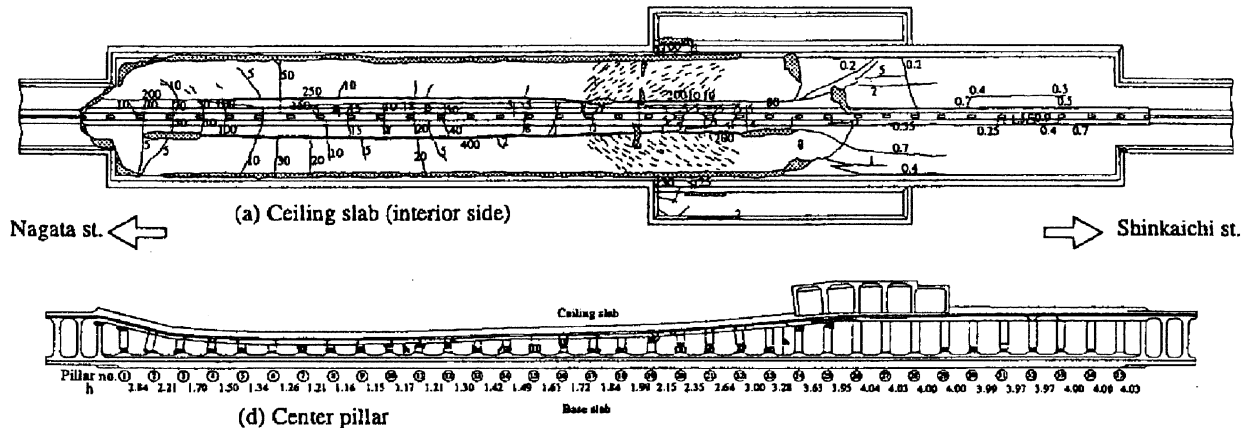
Fig. 2. Section sketch of damage to Daikai subway station (Iida et al., 1996).

2.1.2. Alameda Tubes, Oakland-Alameda, CA, USA

The Alameda Tubes are a pair of immersed-tube tunnels that connect Alameda Island to Oakland in the San Francisco Bay Area. These were some of the earliest immersed tube tunnels built in 1927 and 1963 without seismic design considerations. During the Loma Prieta Earthquake, the ventilation buildings experienced some structural cracking. Limited water leakage into the tunnels was also observed, as was liquefaction of loose deposits above the tube at the Alameda portal. Peak horizontal ground accelerations measured in the area ranged between 0.1 and 0.25 g (EERI, 1990). The tunnels, however, are prone to floatation due to potential liquefaction of the backfill (Schmidt and Hashash, 1998).

2.1.3. L.A. Metro, Los Angeles, CA, USA

The Los Angeles Metro is being constructed in several phases, some of which were operational during the 1994 Northridge Earthquake. The concrete lining of the bored tunnels remained intact after the earthquake. While there was damage to water pipelines, highway bridges and buildings, the earthquake caused no damage to the Metro system. Peak horizontal ground accelerations measured near the tunnels ranged between 0.1 and 0.25 g, with vertical ground accelerations typically two-thirds as large (EERI, 1995).

2.2. Underground structures in Kobe, Japan

The 1995 Hyogoken-Nambu Earthquake caused a major collapse of the Daikai subway station in Kobe, Japan (Nakamura et al., 1996). The station design in 1962 did not include specific seismic provisions. It represents the first modern underground structure to fail during a seismic event. Fig. 2 shows the collapse experienced by the center columns of the station, which was accompanied by the collapse of the ceiling slab and the settlement of the soil cover by more than 2.5 m.

During the earthquake, transverse walls at the ends

of the station and at areas where the station changed width acted as shear walls in resisting collapse of the structure (Iida et al., 1996). These walls suffered significant cracking, but the interior columns in these regions did not suffer as much damage under the horizontal shaking. In regions with no transverse walls, collapse of the center columns caused the ceiling slab to kink and cracks 150–250-mm wide appeared in the longitudinal direction. There was also significant separation at some construction joints, and corresponding water leakage through cracks. Few cracks, if any, were observed in the base slab.

Center columns that were designed with very light transverse (shear) reinforcement relative to the main (bending) reinforcement suffered damage ranging from cracking to complete collapse. Center columns with zigzag reinforcement in addition to the hoop steel, as in Fig. 3, did not buckle as much as those without this reinforcement.

According to Iida et al. (1996), it is likely that the relative displacement between the base and ceiling levels due to subsoil movement created the destructive
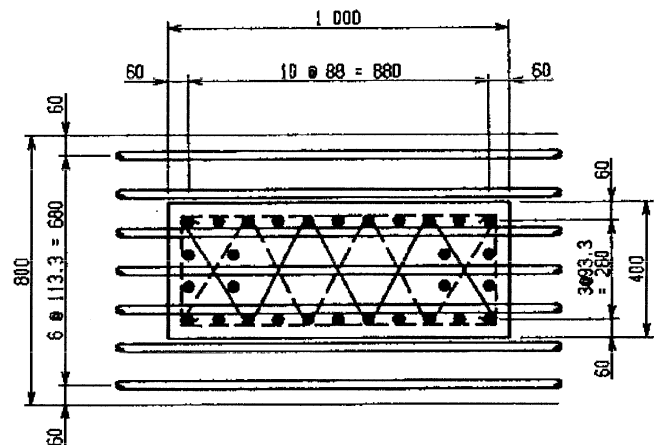

Fig. 3. Reinforcing steel arrangement in center columns (Iida et al., 1996).

horizontal force. This type of movement may have minor effect in a small structure, but in a large one such as a subway station it can be significant. The non-linear behavior of the subsoil profile may also be significant. It is further hypothesized that the thickness of the overburden soil affected the extent of damage between sections of the station by adding inertial force to the structure. Others attribute the failure to high levels of vertical acceleration.

EQE (1995) made further observations about Daikai Station: 'Excessive deflection of the roof slab would normally be resisted by: (1) diaphragm action of the slab, supported by the end walls of the station; and (2) passive earth pressure of the surrounding soils, mobilized as the tube racks. Diaphragm action was less than anticipated, however, due to the length of the station. The method of construction (cut-and-cover, involving a sheet pile wall supported excavation with narrow clearance between the sheet pile wall and the tube wall) made compaction of backfill difficult to impossible, resulting in the tube's inability to mobilize passive earth pressures. In effect, the tube behaved almost as a freestanding structure with little or no extra support from passive earth pressure.' However, it is not certain that good compaction would have prevented the structural failure of the column. Shear failure of supporting columns caused similar damage to the Shinkansen Tunnel through Rokko Mountain (NCEER, 1995).

Several key elements may have helped in limiting the damage to the station structure and possibly prevented complete collapse. Transverse walls at the ends of the station and at areas where the station changed width provided resistance to dynamic forces in the horizontal direction. Center columns with relatively heavy transverse (shear) reinforcement suffered less damage and helped to maintain the integrity of the structure. The
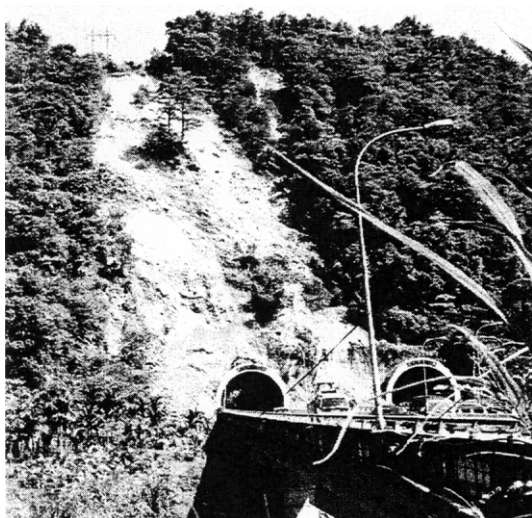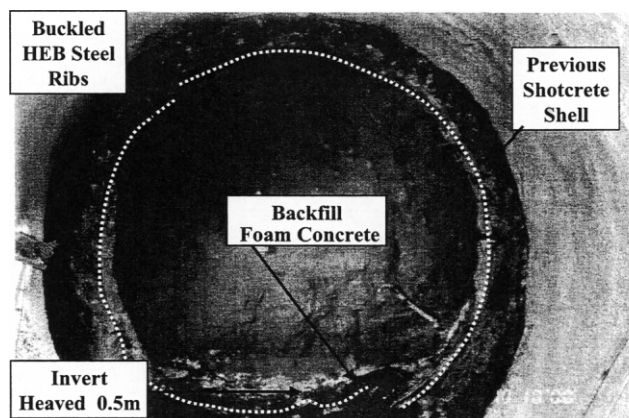

Fig. 5. Bolu Tunnel, re-mining of Bench Pilot Tunnels, showing typical floor heave and buckled steel rib and shotcrete shell (Menkiti, 2001).

fact that the structure was underground instead of being a surface structure may have reduced the amount of related damage.

A number of large diameter (2.0–2.4 m) concrete sewer pipes suffered longitudinal cracking during the Kobe Earthquake, indicating racking and/or compressive failures in the cross-sections (Tohda, 1996). These cracks were observed in pipelines constructed by both the jacking method and open-excavation (cut-and-cover) methods. Once cracked, the pipes behaved as four-hinged arches and allowed significant water leakage.

2.3. Underground structures in Taiwan

Several highway tunnels were located within the zone heavily affected by the September 21, 1999 Chi Chi earthquake (M_L 7.3) in central Taiwan. These are large horseshoe shaped tunnels in rock. All the tunnels inspected by the first author were intact without any visible signs of damage. The main damage occurred at tunnel portals because of slope instability as illustrated in Fig. 4. Minor cracking and spalling was observed in some tunnel lining. One tunnel passing through the Chelungpu fault was shut down because of a 4-m fault movement (Ueng et al., 2001). No damage was reported in the Taipei subway, which is located over 100 km from the ruptured fault zone.

2.4. Bolu Tunnel, Turkey

The twin tunnels are part of a 1.5 billion dollar project that aims at improving transportation in the mountainous terrain to the west of Bolu between Istanbul and Ankara (http://geoinfo.usc.edu/gees). Each tunnel was constructed using the New Austrian Tunneling Method (NATM) where continuous monitoring of primary liner convergence is performed and support

Fig. 4. Slope Failure at Tunnel Portal, Chi-Chi Earthquake, Central Taiwan.

elements are added until a stable system is established. The tunnel has an excavated arch section 15 m tall by 16 m wide. Construction has been unusually challenging because the alignment crosses several minor faults parallel to the North Anatolian Fault. The August 17, 1999 Koceali earthquake was reported to have had minimal impact on the Bolu tunnel. The closure rate of one monitoring station was reported to have temporarily increased for a period of approximately 1 week, then became stable again. Additionally, several hairline cracks, which had previously been observed in the final lining, were being continuously monitored for additional movement and showed no movement due to the earthquake. The November 12, 1999 earthquake caused the collapse of both tunnels 300 m from their eastern portal. At the time of the earthquake, a 800-m section had been excavated, and a 300-m section of unreinforced concrete lining had been completed. The collapse took place in clay gauge material in the unfinished section of the tunnel. The section was covered with shotcrete (sprayed concrete) and had bolt anchors. Fig. 5 shows a section of the collapsed tunnel after it has been re-excavated. Several mechanisms have been proposed for explaining the collapse of the tunnel. These mechanisms include strong ground motion, displacement across the gauge material, and landslide. O'Rourke et al. (2001) present a detailed description of the tunnel performance.

2.5. Summary of seismic performance of underground structures

The Daikai subway station collapse was the first collapse of an urban underground structure due to earthquake forces, rather than ground instability. Underground structures in the US have experienced limited damage during the Loma Prieta and Northridge earthquakes, but the shaking levels have been much lower than the maximum anticipated events. Greater levels of damage can be expected during these maximum events. Station collapse and anticipated strong motions in major US urban areas raise great concerns regarding the performance of underground structures. It is therefore necessary to explicitly account for seismic loading in the design of underground structures.

The data show that in general, damage to tunnels is greatly reduced with increased overburden, and damage is greater in soils than in competent rock. Damage to pipelines (buckling, flotation) was greater than to rail or highway tunnels in both Kobe and Northridge. The major reason for this difference seems to have been the greater thickness of the lining of transportation tunnels. Experience has further shown that cut-and-cover tunnels are more vulnerable to earthquake damage than are circular bored tunnels.

3. Engineering approach to seismic analysis and design

Earthquake effects on underground structures can be grouped into two categories: (1) ground shaking; and (2) ground failure such as liquefaction, fault displacement, and slope instability. Ground shaking, which is the primary focus of this report, refers to the deformation of the ground produced by seismic waves propagating through the earth's crust. The major factors influencing shaking damage include: (1) the shape, dimensions and depth of the structure; (2) the properties of the surrounding soil or rock; (3) the properties of the structure; and (4) the severity of the ground shaking (Dowding and Rozen, 1978; St. John and Zahrah, 1987).

Seismic design of underground structures is unique in several ways. For most underground structures, the inertia of the surrounding soil is large relative to the inertia of the structure. Measurements made by Okamoto et al. (1973) of the seismic response of an immersed tube tunnel during several earthquakes show that the response of a tunnel is dominated by the surrounding ground response and not the inertial properties of the tunnel structure itself. The focus of underground seismic design, therefore, is on the free-field deformation of the ground and its interaction with the structure. The emphasis on displacement is in stark contrast to the design of surface structures, which focuses on inertial effects of the structure itself. This led to the development of design methods such as the Seismic Deformation Method that explicitly considers the seismic deformation of the ground. For example, Kawashima, (1999) presents a review on the seismic behavior and design of underground structures in soft ground with an emphasis on the development of the Seismic Deformation Method.

The behavior of a tunnel is sometimes approximated to that of an elastic beam subject to deformations imposed by the surrounding ground. Three types of deformations (Owen and Scholl, 1981) express the response of underground structures to seismic motions: (1) axial compression and extension (Fig. 6a,b); (2) longitudinal bending (Fig. 6c,d); and (3) ovaling/racking (Fig. 6e,f). Axial deformations in tunnels are generated by the components of seismic waves that produce motions parallel to the axis of the tunnel and cause alternating compression and tension. Bending deformations are caused by the components of seismic waves producing particle motions perpendicular to the longitudinal axis. Design considerations for axial and bending deformations are generally in the direction along the tunnel axis (Wang, 1993).

Ovaling or racking deformations in a tunnel structure develop when shear waves propagate normal or
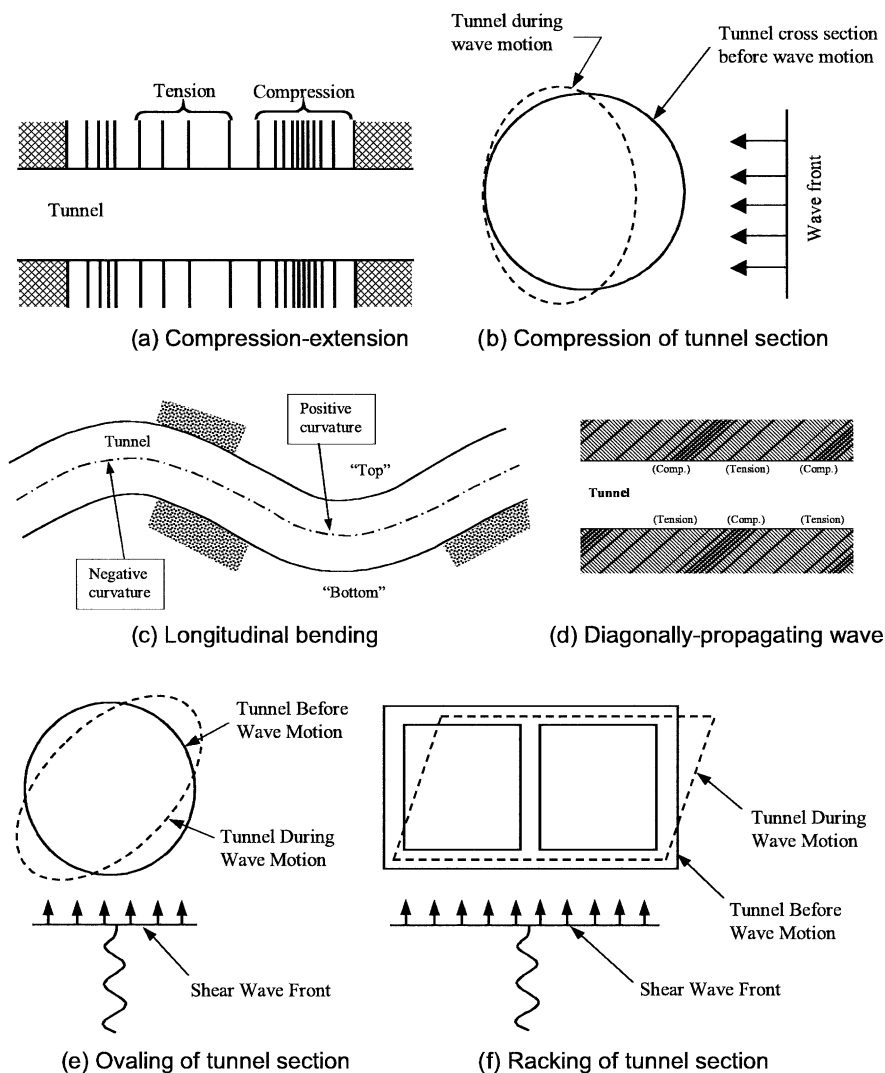
Fig. 6. Deformation modes of tunnels due to seismic waves (after Owen and Scholl, 1981).

nearly normal to the tunnel axis, resulting in a distortion of the cross-sectional shape of the tunnel lining. Design considerations for this type of deformation are in the transverse direction. The general behavior of the lining may be simulated as a buried structure subject to ground deformations under a two-dimensional plane-strain condition.

Diagonally propagating waves subject different parts of the structure to out-of-phase displacements (Fig. 6d), resulting in a longitudinal compression–rarefaction wave traveling along the structure. In general, larger displacement amplitudes are associated with longer wavelengths, while maximum curvatures are produced by shorter wavelengths with relatively small displacement amplitudes (Kuesel, 1969).
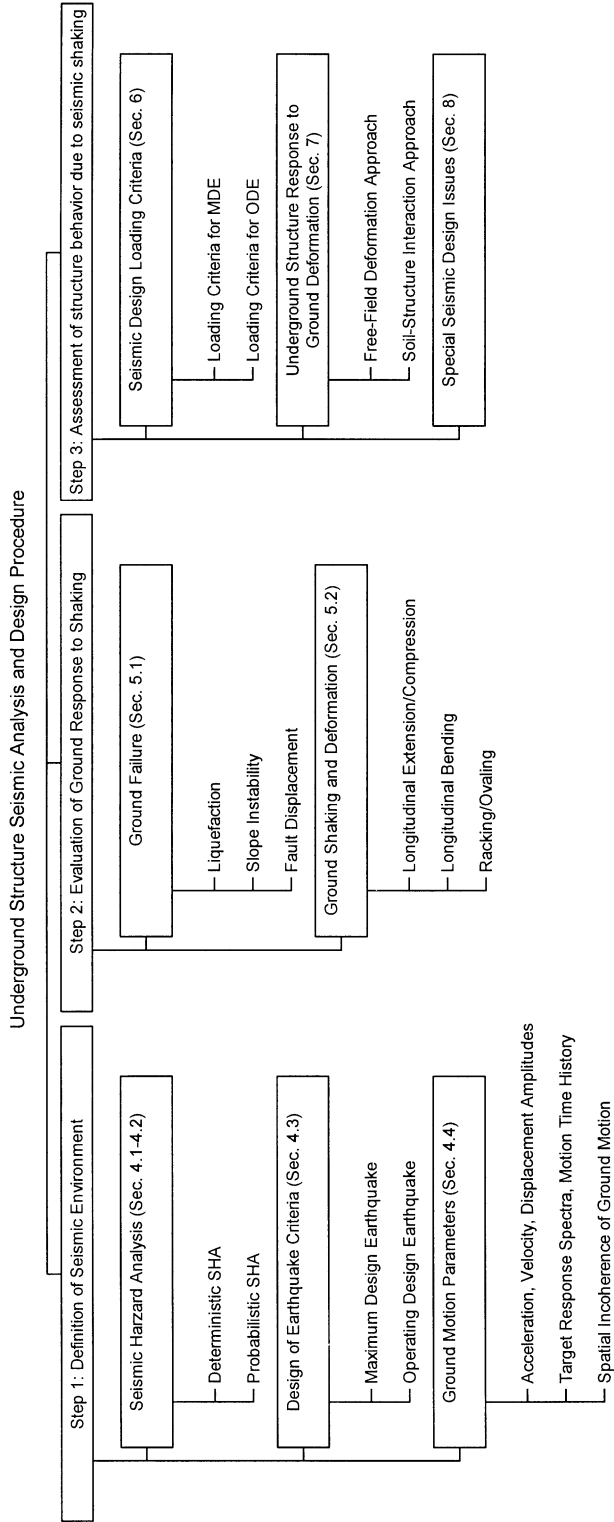
The assessment of underground structure seismic response, therefore, requires an understanding of the anticipated ground shaking as well as an evaluation of the response of the ground and the structure to such shaking. Table 1 summarizes a systematic approach for evaluating the seismic response of underground structures. This approach consists of three major steps:

1. Definition of the seismic environment and development of the seismic parameters for analysis.
2. Evaluation of ground response to shaking, which includes ground failure and ground deformations.
3. Assessment of structure behavior due to seismic shaking including (a) development of seismic design loading criteria, (b) underground structure response to ground deformations, and (c) special seismic design issues.

Steps 1 and 2 are described in Sections 4 and 5, respectively. Sections 6–8 provide the details of Steps 3a, 3b and 3c.
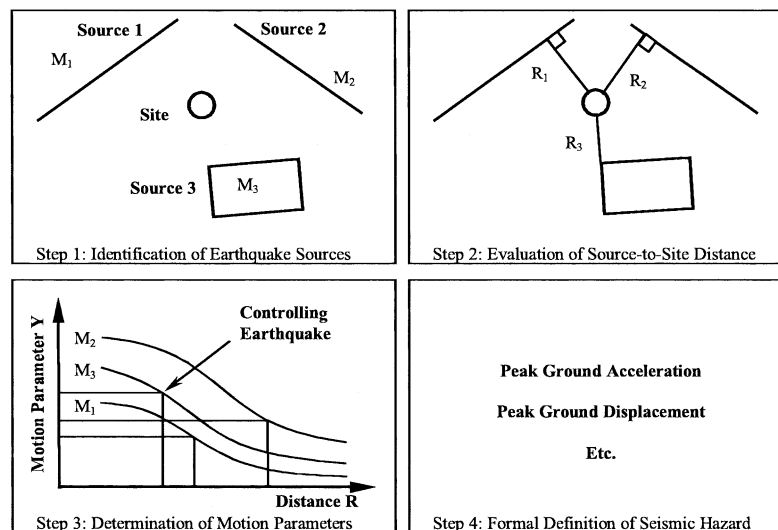
Table 1
Seismic analysis and design procedure

Underground Structure Seismic Analysis and Design Procedure

Step 1: Definition of Seismic Environment

- Seismic Hazard Analysis (Sec. 4.1-4.2)
  - Deterministic SHA
  - Probabilistic SHA
- Design of Earthquake Criteria (Sec. 4.3)
  - Maximum Design Earthquake
  - Operating Design Earthquake
- Ground Motion Parameters (Sec. 4.4)
  - Acceleration, Velocity, Displacement Amplitudes
  - Target Response Spectra, Motion Time History
  - Spatial Incoherence of Ground Motion

Step 2: Evaluation of Ground Response to Shaking

- Ground Failure (Sec. 5.1)
  - Liquefaction
  - Slope Instability
  - Fault Displacement
- Ground Shaking and Deformation (Sec. 5.2)
  - Longitudinal Extension/Compression
  - Longitudinal Bending
  - Racking/Ovaling

Step 3: Assessment of structure behavior due to seismic shaking

- Seismic Design Loading Criteria (Sec. 6)
  - Loading Criteria for MDE
  - Loading Criteria for ODE
- Underground Structure Response to Ground Deformation (Sec. 7)
  - Free-Field Deformation Approach
  - Soil-Structure Interaction Approach
- Special Seismic Design Issues (Sec. 8)

Fig. 7. Deterministic seismic hazard analysis procedure (after Reiter, 1990).

4. Definition of seismic environment

The goal of earthquake-resistant design for underground structures is to develop a facility that can withstand a given level of seismic motion with damage not exceeding a pre-defined acceptable level. The design level of shaking is typically defined by a design ground motion, which is characterized by the amplitudes and characteristics of expected ground motions and their expected return frequency (Kramer, 1996). A seismic hazard analysis is used to define the level of shaking and the design earthquake(s) for an underground facility.

A seismic hazard analysis typically characterizes the potential for strong ground motions by examining the extent of active faulting in a region, the potential for fault motion, and the frequency with which the faults release stored energy. This examination may be difficult in some regions (e.g. Eastern USA) where faulting is not readily detectable. There are two methods of analysis: (a) the deterministic seismic hazard analysis (DSHA); and (b) the probabilistic seismic hazard analysis (PSHA). A deterministic seismic hazard analysis develops one or more earthquake motions for a site, for which the designers then design and evaluate the underground structure. The more recent probabilistic seismic hazard analysis, which explicitly quantifies the uncertainties in the analysis, develops a range of expected ground motions and their probabilities of occurrence. These probabilities can then be used to determine the level of seismic protection in a design.

4.1. Deterministic seismic hazard analysis (DSHA)

A deterministic seismic hazard analysis involves the development of a particular seismic scenario to sum-

marize the ground motion hazard at a site. This scenario requires the 'postulated occurrence' of a particular size of earthquake at a particular location. Reiter (1990) outlined the following four-step process (see Fig. 7):

1. Identification and characterization of all earthquake sources capable of producing significant ground motion at the site, including definition of the geometry and earthquake potential of each. The most obvious feature delineating a seismic zone is typically the presence of faulting. Reiter (1990) generated a comprehensive list of features that may suggest faulting in a given region. However, the mere presence of a fault does not necessarily signify a potential earthquake hazard — the fault must be active to present a risk. There has been considerable disagreement over the criteria for declaring a fault active or inactive. Rather than using the term 'active', the US Nuclear Regulatory Commission (Code of Federal Regulations, 1978) coined the term capable fault to indicate a fault that has shown activity within the past 35 000–500 000 years. For non-nuclear civil infrastructure, shorter timeframes would be used.

2. Selection of a source-to-site distance parameter for each source, typically the shortest epicentral/hypocentral distance or the distance to the closest ruptured portion of the fault. Closest distance to ruptured fault is more meaningful than epicentral distance especially for large earthquakes where the ruptured fault extends over distances exceeding 50 km.

3. Selection of a controlling earthquake (i.e. that which produces the strongest shaking level at the site), generally expressed in terms of a ground

motion parameter at the site. Attenuation relationships are typically used to determine these site-specific parameters from data recorded at nearby locations. Several studies have attempted to correlate earthquake magnitudes, most commonly moment magnitudes, with observed fault deformation characteristics, such as rupture length and area, and have found a strong correlation. However, the unavailability of fault displacement measurements over the entire rupture surface severely limits our ability to measure these characteristics. Instead, researchers have tried to correlate the maximum surface displacement with magnitude — to varying results. Empirically based relationships, such as those developed by Wells and Coppersmith (1994), can be utilized to estimate these correlations. Another, more basic way to evaluate the potential for seismic activity in a region is through examination of historical records. These records allow engineers to outline and track active faults and their release of seismic potential energy. The evaluation of fore- and aftershocks can also help delineate seismic zones (Kramer, 1996). In addition to the examination of historical records, a study of geologic record of past seismic activities called paleo-seismology can be used to evaluate the occurrence and size of earthquakes in the region. Geomorphic (surface landform) and trench studies may reveal the number of past seismic events, slip per event, and timing of the events at a specific fault. In some cases, radiocarbon (^{14}C) dating of carbonized roots, animal bone fossils or soil horizons near the features of paleoseismic evidence can be utilized to approximate ages of the events.

4. Formal definition of the seismic hazard at the site in terms of the peak acceleration, velocity and displacement, response spectrum ordinates, and ground motion time history of the maximum credible earthquake. Design fault displacements should also be defined, if applicable.

A DSHA provides a straightforward framework for the evaluation of worst-case scenarios at a site. However, it provides no information about the likelihood or frequency of occurrence of the controlling earthquake. If such information is required, a probabilistic approach must be undertaken to better quantify the seismic hazard.

4.2. Probabilistic seismic hazard analysis (PSHA)

A probabilistic seismic hazard analysis provides a framework in which uncertainties in the size, location, and recurrence rate of earthquakes can be identified, quantified, and combined in a rational manner. Such an analysis provides designers with a more complete description of the seismic hazard at a site, where variations in ground motion characteristics can be explicitly considered. For this type of analysis, future earthquake events are assumed spatially and temporally independent. Reiter (1990) outlined the four major steps involved in PSHA (see Fig. 8):

1. Identification and characterization of earthquake sources, including the probability distribution of potential rupture locations within the source zone. These distributions are then combined with the source geometry to obtain the probability distribution of source-to-site distances. In many regions throughout the world, including the USA, specific active fault zones often cannot be identified. In
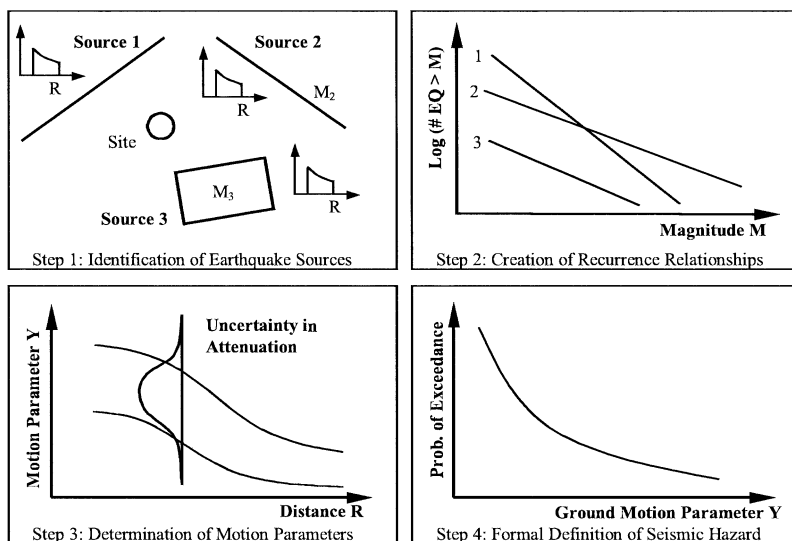

Fig. 8. Probabilistic seismic hazard analysis procedure (after Reiter, 1990).

these cases, seismic history and geological considerations become critical for hazard analyses.

2. Characterization of the seismicity or temporal distribution of earthquake recurrence. Information obtained from historical data and paleoseismological studies can help to develop a recurrence relationship that describes the average rate at which an earthquake of certain size will be exceeded.

3. Determination of the ground motion produced at the site by any size earthquake occurring at any source zone using attenuation relationships. The uncertainty inherent in the predictive relationship is also considered.

4. Combination of these uncertainties to obtain the probability that a given ground motion parameter will be exceeded during a given time period.

The probabilistic approach incorporates the uncertainties in source-to-site distance, magnitude, rate of recurrence and the variation of ground motion characteristics into the analyses. In areas where no active faults can be readily identified it may be necessary to rely on a purely statistical analysis of historic earthquakes in the region. The details of this procedure are beyond the scope of this report.

4.3. Design earthquakes criteria

Once the seismic hazard at the site is characterized, the level of design earthquake or seismicity has to be defined. For example, in PSHA, the designer must select the probability of exceedance for the sets of ground motion parameters. Current seismic design philosophy for many critical facilities requires dual (two-level) design criteria, with a higher design level earthquake aimed at life safety and a lower design level earthquake intended for economic risk exposure. The two design levels are commonly defined as 'maximum design earthquake' (or 'safety evaluation earthquake') and 'operational design earthquake' (or 'function evaluation earthquake'), and have been employed in many recent transportation tunnel projects, including the Los Angeles Metro, Taipei Metro, Seattle Metro, and Boston Central Artery/Third Harbor Tunnels.

4.3.1. Maximum Design Earthquake

The Maximum Design Earthquake (MDE) is defined in a DSHA as the maximum level of shaking that can be experienced at the site. In a PSHA, the MDE is defined as an event with a small probability of exceedance during the life of the facility (e.g. 3–5%). The MDE design goal is that public safety shall be maintained during and after the design event, meaning that the required structural capacity under an MDE loading must consider the worst-case combination of live, dead, and earthquake loads. Recently, some owners (e.g. San

Francisco BART) have begun requiring their facilities, identified as lifelines, to remain operational after MDE level shaking.

4.3.2. Operating Design Earthquake

The Operating Design Earthquake (ODE) is an earthquake event that can be reasonably expected to occur at least once during the design life of the facility (e.g. an event with probability of exceedence between 40 and 50%). In an ODE analysis, the seismic design loading depends on the structural performance requirements of the structural members. Since the ODE design goal is that the overall system shall continue operating during and after an ODE and experience little or no damage, inelastic deformations must be kept to a minimum. The response of the underground facility should therefore remain within the elastic range.

4.4. Ground motion parameters

Once an MDE or ODE is defined, sets of ground motion parameters are required to characterize the design events. The choice of these parameters is related to the type of analysis method used in design. At a particular point in the ground or on a structure, ground motions can be described by three translational components and three rotational components, though rotational components are typically ignored. A ground motion component is characterized by a time history of acceleration, velocity or displacement with three significant parameters: amplitude; frequency content; and duration of strong ground motion.

4.4.1. Acceleration, velocity, and displacement amplitudes

Maximum values of ground motion such as peak ground acceleration, velocity and displacement are commonly used in defining the MDE and ODE developed through seismic hazard analysis. However, experience has shown that effective, rather than peak, ground motion parameters tend to be better indicators of structural response, as they are more representative of the damage potential of a given ground motion. This is especially true for large earthquakes. The effective value is sometimes defined as the sustained level of shaking, and computed as the third or fifth highest value of the parameter (Nuttli, 1979). Earthquake damage to underground structures has also proven to be better correlated with particle velocity and displacement than acceleration. Attenuation relationships are generally available for estimating peak ground surface accelerations, but are also available for estimating peak velocities and displacements. Tables 2 and 3 can be used to relate the known peak ground acceleration to estimates of peak ground velocity and displacement, respectively, in the absence of site-specific data.

Table 2
Ratios of peak ground velocity to peak ground acceleration at surface in rock and soil (after Power et al., 1996)

Moment magnitude (M_w)	Ratio of peak ground velocity (cm/s) to peak ground acceleration (g)		
	Source-to-site distance (km)		
	0–20	20–50	50–100
Rock[a]			
6.5	66	76	86
7.5	97	109	97
8.5	127	140	152
Stiff soil[a]			
6.5	94	102	109
7.5	140	127	155
8.5	180	188	193
Soft soil[a]			
6.5	140	132	142
7.5	208	165	201
8.5	269	244	251

[a] In this table, the sediment types represent the following shear wave velocity ranges: rock ≥ 750 m/s; stiff soil is 200–750 m/s; and soft soil < 200 m/s. The relationship between peak ground velocity and peak ground acceleration is less certain in soft soils.

4.4.2. Target response spectra and motion time history

The most common way to express the parameters of a design ground motion is through acceleration response spectra, which represents the response of a damped single degree of freedom system to ground motion. Once a target response spectrum has been

Table 3
Ratios of peak ground displacement to peak ground acceleration at surface in rock and soil (after Power et al., 1996)

Moment magnitude (M_w)	Ratio of peak ground displacement (cm) to peak ground acceleration (g)		
	Source-to-site distance (km)		
	0–20	20–50	50–100
Rock[a]			
6.5	18	23	30
7.5	43	56	69
8.5	81	99	119
Stiff soil[a]			
6.5	35	41	48
7.5	89	99	112
8.5	165	178	191
Soft soil[a]			
6.5	71	74	76
7.5	178	178	178
8.5	330	320	305

[a] In this table, the sediment types represent the following shear wave velocity ranges: rock ≥ 750 m/s; stiff soil is 200–750 m/s; and soft soil < 200 m/s. The relationship between peak ground velocity and peak ground acceleration is less certain in soft soils.

chosen, one or more ground motion time histories may be developed that match the design response spectra. These time histories can be either synthetic or based on actual recordings of earthquakes with similar characteristics.

While the response spectrum is a useful tool for the designer, it should not be used if (1) the soil-structure system response is highly non-linear, or (2) the structure is sufficiently long that the motion could vary significantly in amplitude and phase along its length. In these cases, time histories (St. John and Zahrah, 1987) combined with local site response analysis are typically more useful.

4.4.3. Spatial incoherence of ground motion

For many engineering structures, the longest dimension of the structure is small enough that the ground motion at one end is virtually the same as that at the other end. However, for long structures such as bridges or tunnels, different ground motions may be encountered by different parts of the structure and traveling wave effects must be considered (Hwang and Lysmer, 1981). This spatial incoherence may have a significant impact on the response of the structure. There are four major factors that may cause spatial incoherence: (1) wave-passage effects; (2) extended source effects; (3) ray-path effects caused by inhomogeneities along the travel path; and (4) local soil site effects. The reader should refer to Hwang and Lysmer (1981) for details on these factors. Recorded ground motions have shown that spatial coherency decreases with increasing distance and frequency (Kramer, 1996). The generation of ground motion time histories with appropriate spatial incoherence is a critical task if the designer is to compute differential strains and force buildup along a tunnel length. The designer will have to work closely with an engineering seismologist to identify the relevant factors contributing to ground motion incoherence at a specific site and to generate appropriate ground motion time histories. Hashash et al. (1998) show how the use of time histories with spatial incoherence affects the estimation of axial force development in a tunnel and can lead to significant longitudinal push-pull and other effects.

4.5. Wave propagation and site-specific response analysis

Research has shown that transverse shear waves transmit the greatest proportion of the earthquake's energy, and amplitudes in the vertical plane have been typically estimated to be a half to two-thirds as great as those in the horizontal plane. However, in recent earthquakes such as Northridge and Kobe, measured vertical accelerations were equal to and sometimes larger than horizontal accelerations. Vertical compo-

nent of ground motion has become an important issue in seismic designs.

Ample strong ground motion data are generally not available at the depths of concern for underground structures, so the development of design ground motions needs to incorporate depth-dependent attenuation effects. Popular analytical procedures use one-dimensional site response techniques, although these analyses ignore the effects of all but vertically propagating body waves. One method, discussed by Schnabel, et al. (1972), applies a deconvolution procedure to a surface input motion in order to evaluate the motion at depth. A second method involves applying ground motions at various depths to find the scale factors necessary to match the input motion. Both of these procedures are repeated for a collection of soil properties and ground motions to develop a 'ground motion spectrum' for the site (St. John and Zahrah, 1987). Linear, equivalent linear (SHAKE, Schnabel et al., 1972) or non-linear (Hashash and Park, 2001; Borja et al., 1999, D-MOD, Matasovic and Vucetic, 1995, Cyberquake, BRGM, 1998, Desra, Finn et al., 1977) one-dimensional wave propagation methods are commonly used to propagate waves through soft soil deposits. Ground motions generally decrease with depth (e.g. Chang et al., 1986). Performing a wave propagation analysis is needed as the amplitude and period of vibration of the ground motion shift as the shear wave passes through soft soil deposits. In the absence of more accurate (numerical) methods or data, Table 4 can be used to determine the relationship between ground motion at depth and that at the ground surface.

5. Evaluation of ground response to shaking

The evaluation of ground response to shaking can be divided into two groups: (1) ground failure; and (2) ground shaking and deformation. This report focuses on ground shaking and deformation, which assumes that the ground does not undergo large permanent displacements. A brief overview of issues related to ground failure are also presented.

5.1. Ground failure

Ground failure as a result of seismic shaking includes liquefaction, slope instability, and fault displacement. Ground failure is particularly prevalent at tunnel portals and in shallow tunnels. Special design considerations are required for cases where ground failure is involved, and are discussed in Section 8.

5.1.1. Liquefaction
Liquefaction is a term associated with a host of different, but related phenomena. It is used to describe

Table 4
Ratios of ground motion at depth to motion at ground surface (after Power et al., 1996)

Tunnel depth (m)	Ratio of ground motion at tunnel depth to motion at ground surface
≤ 6	1.0
6–15	0.9
15–30	0.8
> 30	0.7

the phenomena associated with increase of pore water pressure and reduction in effective stresses in saturated cohesionless soils. The rise in pore pressure can result in generation of sand boils, loss of shear strength, lateral spreading and slope failure. The phenomena are more prevalent in relatively loose sands and artificial fill deposits.

Tunnels located below the groundwater table in liquefiable deposits can experience (a) increased lateral pressure, (b) a loss of lateral passive resistance, (c) flotation or sinking in the liquefied soil, (d) lateral displacements if the ground experiences lateral spreading, and (e) permanent settlement and compression and tension failure after the dissipation of pore pressure and consolidation of the soil.

5.1.2. Slope instability
Landsliding as a result of ground shaking is a common phenomena. Landsliding across a tunnel can result in concentrated shearing displacements and collapse of the cross section. Landslide potential is greatest when a pre-existing landslide mass intersects the tunnel. The hazard of landsliding is greatest in shallower parts of a tunnel alignment and at tunnel portals.

At tunnel portals, the primary failure mode tends to be slope failures. Particular caution must be taken if the portal also acts as a retaining wall (St. John and Zahrah, 1987). During the September 21, 1999 Chi Chi earthquake in Taiwan slope instability at tunnel portals was very common, e.g. Fig. 4.

5.1.3. Fault displacement
An underground structure may have to be constructed across a fault zone as it is not always possible to avoid crossing active faults. In these situations, the underground structure must tolerate the expected fault displacements, and allow only minor damages. All faults must be identified to limit the length of special design section, and a risk-cost analysis should be run to determine if the design should be pursued.

5.2. Ground shaking and deformation

In the absence of ground failure that results in large

permanent deformation, the design focus shifts to the transient ground deformation induced by seismic wave passage. The deformation can be quite complex due to the interaction of seismic waves with surficial soft deposits and the generation of surface waves. For engineering design purposes, these complex deformation modes are simplified into their primary modes. Underground structures can be assumed to undergo three primary modes of deformation during seismic shaking: (1) compression–extension; (2) longitudinal bending; and (3) ovalling/racking (Fig. 6). The simplest mode to consider is that of a compression wave propagating parallel to the axis of a subsurface excavation. That case is illustrated in the figure, where the wave is shown inducing longitudinal compression and tension. The case of an underground structure subjected to an axially propagating wave is slightly more complex since there will be some interaction between the structure and the ground. This interaction becomes more important if the ground is soft and shear stress transfer between the ground and the structure is limited by the interface shear strength. For the case of a wave propagating normal or transverse to the tunnel axis, the stress induces shear deformations of the cross section called racking or ovaling. In the more general case, the wave may induce curvature in the structure, inducing alternate regions of compression and tension along the tunnel. The beam-like structure of the tunnel lining will then experience tension and compression on opposite sides.

6. Seismic design loading criteria

Design loading criteria for underground structures has to incorporate the additional loading imposed by ground shaking and deformation. Once the ground motion parameters for the maximum and operational design earthquakes have been determined, load criteria are developed for the underground structure using the load factor design method. This section presents the seismic design loading criteria (Wang, 1993) for MDE and ODE.

6.1. Loading criteria for maximum design earthquake, MDE

Given the performance goals of the MDE (Section 4.3.1), the recommended seismic loading combinations using the load factor design method are as follows:

6.1.1. For cut-and-cover tunnel structures

$$U = D + L + E1 + E2 + EQ \qquad (1)$$

where U = required structural strength capacity, D =

effects due to dead loads of structural components, L = effects due to live loads, $E1$ = effects due to vertical loads of earth and water, $E2$ = effects due to horizontal loads of earth and water and EQ = effects due to design earthquake motion.

6.1.2. For bored or mined (circular) tunnel lining

$$U = D + L + EX + H + EQ \qquad (2)$$

where U, D, L and EQ are as defined in Eq. (1), EX = effects of static loads due to excavation (e.g. O'Rourke, 1984), and H = effects due to hydrostatic water pressure.

6.1.3. Comments on loading combinations for MDE

- The structure should first be designed with adequate strength capacity under static loading conditions.
- The structure should then be checked in terms of ductility (its allowable deformation vs. maximum deformation imposed by earthquake) as well as strength when earthquake effects, EQ, are considered. The 'EQ' term for conventional surface structure design reflects primarily the inertial effect on the structures. For tunnel structures, the earthquake effect is governed not so much by a force or stress, but rather by the deformation imposed by the ground.
- In checking the strength capacity, the effects of earthquake loading should be expressed in terms of internal moments and forces, which can be calculated according to the lining deformations imposed by the surrounding ground. If the 'strength' criteria expressed by Eq. (1) or Eq. (2) can be satisfied based on elastic structural analysis, no further provisions under the MDE are required. Generally, the strength criteria can easily be met when the earthquake loading intensity is low (i.e. in low seismic risk areas) and/or the ground is very stiff.
- If the flexural strength of the structure lining, using elastic analysis and Eq. (1) or Eq. (2), is found to be exceeded (e.g. at certain joints of a cut-and-cover tunnel frame), one of the following two design procedures should be followed:
1. Provide sufficient ductility (using appropriate detailing procedure) at the critical locations of the structure to accommodate the deformations imposed by the ground in addition to those caused by other loading effects (see Eqs. (1) and (2)). The intent is to ensure that the structural strength does not degrade as a result of inelastic deformations and the damage can be controlled at an acceptable level.

    In general, the more ductility that is provided, the more reduction in earthquake forces (the 'EQ'

term) can be made in evaluating the required strength, *U*. As a rule of thumb, the force reduction factor can be assumed equal to the ductility (factor) provided. This reduction factor is similar by definition to the response modification factor used in bridge design code (AASHTO, 1991).

Note, however, that since an inelastic 'shear' deformation may result in strength degradation, it should always be prevented by providing sufficient shear strengths in structure members, particularly in the cut-and-cover rectangular frame. The use of ductility factors for shear forces may not be appropriate.

2. Re-analyze the structure response by assuming the formation of plastic hinges at the joints that are strained into inelastic action. Based on the plastic-hinge analysis, a redistribution of moments and internal forces will result.

If new plastic hinges are developed based on the results, the analysis is re-run by incorporating the new hinges (i.e. an iterative procedure) until all potential plastic hinges are properly accounted for. Proper detailing at the hinges is then carried out to provide adequate ductility. The structural design in terms of required strength (Eqs. (1) and (2)) can then be based on the results from the plastic-hinge analysis.

As discussed earlier, the overall stability of the structure during and after the MDE must be maintained. Realizing that the structures also must have sufficient capacity (besides the earthquake effect) to carry static loads (e.g. *D*, *L*, *E*1, *E*2 and *H* terms), the potential modes of instability due to the development of plastic hinges (or regions of inelastic deformation) should be identified and prevented (Monsees and Merritt, 1991).

- For cut-and-cover tunnel structures, the evaluation of capacity using Eq. (1) should consider the uncertainties associated with the loads *E*1 and *E*2, and their worst combination. For mined circular tunnels (Eq. (2)), similar consideration should be given to the loads *EX* and *H*.
- In many cases, the absence of live load, *L*, may present a more critical condition than when a full live load is considered. Therefore, a live load equal to zero should also be used in checking the structural strength capacity using Eq. (1) and Eq. (2).

6.2. Loading criteria for operating design earthquake, ODE

For the ODE (Section 4.3.2), the seismic design loading combination depends on the performance requirements of the structural members. Generally speaking, if the members are to experience little to no damage during the lower-level event (ODE), the inelastic deformations in the structure members should be kept low. The following loading criteria, based on load factor design, are recommended:

6.2.1. For cut-and-cover tunnel structures

$$U = 1.05D + 1.3L + \beta_1(E1 + E2) + 1.3EQ \qquad (3)$$

Where *D*, *L*, *E*1, *E*2, *EQ* and *U* are as defined in Eq. (1), $\beta_1 = 1.05$ if extreme loads are assumed for *E*1 and *E*2 with little uncertainty. Otherwise, use $\beta_1 = 1.3$.

6.2.2. For bored or mined (circular) tunnel lining

$$U = 1.05D + 1.3L + \beta_2(EX + H) + 1.3EQ \qquad (4)$$

where *D*, *L*, *EX*, *H*, *EQ* and *U* are as defined in Eq. (2), $\beta_2 = 1.05$ if extreme loads are assumed for *EX* and *H* with little uncertainty. Otherwise, use $\beta_2 = 1.3$ for *EX* only, as *H* is usually well defined.

The load factors used in these two equations have been the subject of a lot of discussion. The final selection depends on the project-specific performance requirements. For example, a factor of 1.3 is used for dead load in the Central Artery (I-93)/Tunnel (I-90) Project (Central Artery Project Design Criteria, Bechtel/Parsons Brinckerhoff, 1992).

6.2.3. Comments on loading combinations for ODE

- The structure should first be designed with adequate strength capacity under static loading conditions.
- For cut-and-cover tunnel structures, the evaluation of capacity using Eq. (3) should consider the uncertainties associated with the loads *E*1 and *E*2, and their worst combination. For mined circular tunnels (Eq. (4)), similar consideration should be given to the loads *EX* and *H*.
- When the extreme loads are used for design, a smaller load factor is recommended to avoid unnecessary conservatism. Note that an extreme load may be a maximum load or a minimum load, depending on the most critical case of the loading combinations. Use Eq. (4) as an example. For a deep circular tunnel lining, it is very likely that the most critical loading condition occurs when the maximum excavation loading, *EX*, is combined with the minimum hydrostatic water pressure, *H* (unless *EX* is unsymmetrical). For a cut-and-cover tunnel, the most critical seismic condition may often be found when the maximum lateral earth pressure, *E*2, is combined with the minimum vertical earth load, *E*1. If a very conservative earth pressure

coefficient is assumed in calculating the $E2$, the smaller load factor $\beta_1 = 1.05$ should be used.

- Redistribution of moments (e.g. ACI 318, 1999) for cut-and-cover concrete frames is recommended to achieve a more efficient design.
- If the 'strength' criteria expressed by Eq. (3) or Eq. (4) can be satisfied based on elastic structural analysis, no further provisions under the ODE are required.
- If the flexural strength of the structure, using elastic analysis and Eq. (3) or Eq. (4), is found to be exceeded, the structure should be checked (for its ductility) to ensure that the resulting inelastic deformations, if any, are small. If necessary, the structure should be redesigned to ensure the intended performance goals during the ODE.
- Zero live load condition (i.e. $L = 0$) should also be evaluated in Eq. (3) and Eq. (4).

7. Underground structure response to ground deformations

In this section, the term EQ (effects due to design earthquake) introduced in Section 6 is quantified. The development of the EQ term requires an understanding of the deformations induced by seismic waves in the ground and the interaction of the underground structure with the ground.

This section describes procedures used to compute deformations and forces corresponding to the three deformation modes (compression-extension, longitudinal bending and ovalling/racking) presented in Section 5.2. A brief summary of design approaches is provided in Table 6.

7.1. Free field deformation approach

The term 'free-field deformations' describes ground strains caused by seismic waves in the absence of structures or excavations. These deformations ignore the interaction between the underground structure and the surrounding ground, but can provide a first-order estimate of the anticipated deformation of the structure. A designer may choose to impose these deformations directly on the structure. This approach may overestimate or underestimate structure deformations depending on the rigidity of the structure relative to the ground.

7.1.1. Closed form elastic solutions

Simplified, closed-form solutions are useful for developing initial estimates of strains and deformations in a tunnel. These simplified methods assume the seismic wave field to be that of plane waves with the same amplitudes at all locations along the tunnel, differing only in their arrival time. Wave scattering and complex three-dimensional wave propagation, which can lead to differences in wave amplitudes along the tunnel are neglected, although ground motion incoherence (Section 4.4.3) tends to increase the strains and stresses in the longitudinal direction. Results of analyses based on plane wave assumptions should be interpreted with care (Power et al., 1996).

Newmark (1968) and Kuesel (1969) proposed a simplified method for calculating free-field ground strains caused by a harmonic wave propagating at a given angle of incidence in a homogeneous, isotropic, elastic medium (Fig. 9). The most critical incidence angle yielding maximum strain, is typically used as a safety measure against the uncertainties of earthquake prediction. Newmark's approach provides an order of magnitude estimate of wave-induced strains while requiring a minimal input, making it useful as both an initial design tool and a method of design verification (Wang, 1993).

St. John and Zahrah (1987) used Newmark's approach to develop solutions for free-field axial and curvature strains due to compression, shear and Rayleigh waves. Solutions for all three wave types are shown in Table 5, though S-waves are typically associated with peak particle accelerations and velocities (Power et al., 1996). The seismic waves causing the strains are shown in Fig. 10. It is often difficult to determine which type of wave will dominate a design. Strains produced by Rayleigh waves tend to govern only in shallow structures and at sites far from the seismic source (Wang, 1993).

Combined axial and curvature deformations can be obtained by treating the tunnel as an elastic beam. Using beam theory, total free-field axial strains, (ε^{ab}) are found by combining the longitudinal strains generated by axial and bending deformations (Power et al., 1996):

$$\varepsilon^{ab} = \left[\frac{V_P}{C_P}\cos^2\phi + r\frac{a_P}{C_P^2}\sin\phi\cos^2\phi \right] \tag{5}$$

for P − waves

$$\varepsilon^{ab} = \left[\frac{V_S}{C_S}\sin\phi\cos\phi + r\frac{a_S}{C_S^2}\cos^3\phi \right] \tag{6}$$

for S − waves

$$\varepsilon^{ab} = \left[\frac{V_R}{C_R}\cos^2\phi + r\frac{a_R}{C_R^2}\sin\phi\cos^2\phi \right] \tag{7}$$
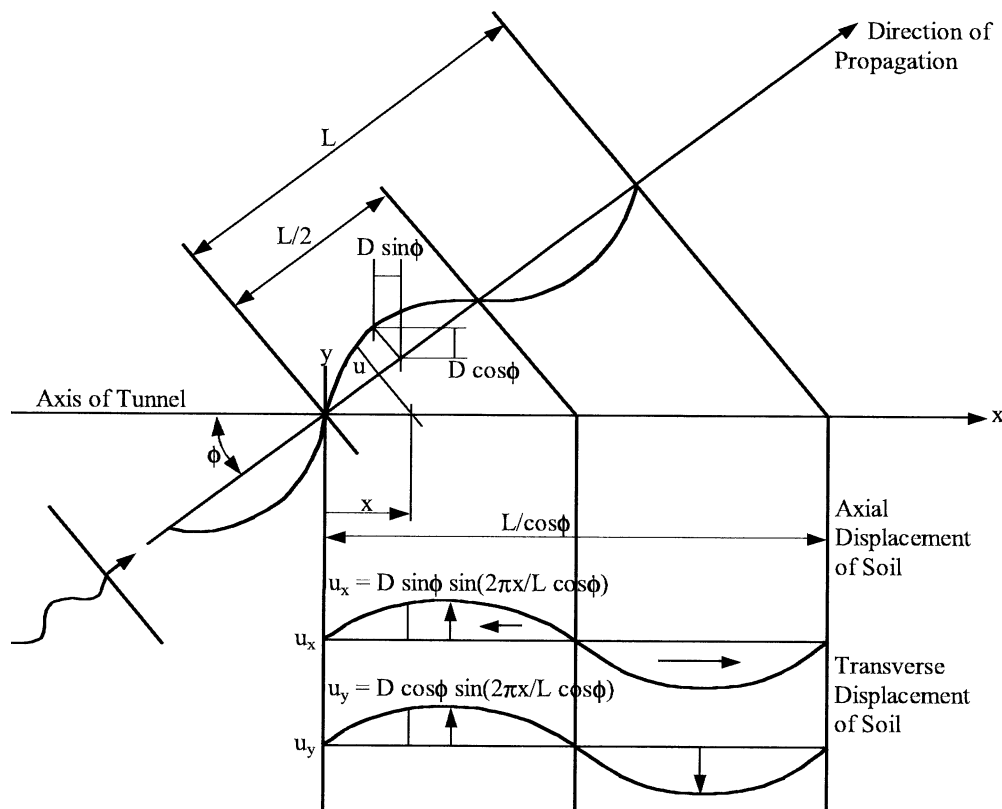
for Rayleigh − waves (compressional component)

Fig. 9. Simple harmonic wave and tunnel (after Wang, 1993).

Where:

r: radius of circular tunnel or half height of a rectangular tunnel

a_P: peak particle acceleration associated with P-wave

a_S: peak particle acceleration associated with S-wave

a_R: peak particle acceleration associated with Rayleigh wave

ϕ: angle of incidence of wave with respect to tunnel axis

ν_l: Poisson's ratio of tunnel lining material

V_p: peak particle velocity associated with P-wave

C_p: apparent velocity of P-wave propagation

V_s: peak particle velocity associated with S-wave

C_s: apparent velocity of S-wave propagation

V_R: peak particle velocity associated with Rayleigh Wave

C_R: apparent velocity of Rayleigh wave propagation

As the radius of the tunnel increases, the contribution of curvature deformation to axial strain increases. However, calculations using the free-field equations of Table 5 indicate that the bending component of strain is, in general, relatively small compared to axial strains for tunnels under seismic loading. The cyclic nature of the axial strains should also be noted — although a tunnel lining may crack in tension, this cracking is usually transient due to the cyclic nature of the incident waves. The reinforcing steel in the lining will close these cracks at the end of the shaking, provided there is no permanent ground deformation (and the steel has not yielded). Even unreinforced concrete linings are considered adequate as long as the cracks are small, uniformly distributed, and do not adversely affect the performance of the lining (Wang, 1993).

It should be noted that the apparent P- and S-wave velocities used in these equations may be closer to those of seismic wave propagation through deep rocks rather than the shallow soil or rock in which a tunnel may be located based on data from Abrahamson (1985, 1992, 1995). The apparent S-wave velocities fall in the range of 2–4 km/s while apparent P-wave velocities fall in the range of 4–8 km/s (Power et al., 1996).

7.1.2. Ovaling deformation of circular tunnels

Ovaling deformations develop when waves propagate perpendicular to the tunnel axis and are therefore, designed for in the transverse direction (typically under two-dimensional, plane-strain conditions). Studies have suggested that, while ovaling may be caused by waves propagating horizontally or obliquely, vertically propagating shear waves are the predominant form of earthquake loading that causes these types of deformations (Wang, 1993).

Table 5
Strain and curvature due to body and surface waves (after St. John and Zahrah, 1987)

Wave type	Longitudinal strain	Normal strain	Shear strain	Curvature
P-wave	$\varepsilon_l = \dfrac{V_P}{C_P}\cos^2\phi$	$\varepsilon_n = \dfrac{V_P}{C_P}\sin^2\phi$	$\gamma = \dfrac{V_P}{C_P}\sin\phi\cos\phi$	$\dfrac{1}{\rho} = \dfrac{a_P}{C_P^2}\sin\phi\cos^2\phi$
	$\varepsilon_{lm} = \dfrac{V_P}{C_P}$ for $\phi = 0°$	$\varepsilon_{lm} = \dfrac{V_P}{C_P}$ for $\phi = 90°$	$\gamma_m = \dfrac{V_P}{2C_P}$ for $\phi = 45°$	$\dfrac{1}{\rho_{max}} = 0.385\dfrac{a_P}{C_P^2}$ for $\phi = 35°16'$
S-wave	$\varepsilon_l = \dfrac{V_S}{C_S}\sin\phi\cos\phi$	$\varepsilon_n = \dfrac{V_S}{C_S}\sin\phi\cos\phi$	$\gamma = \dfrac{V_S}{C_S}\cos^2\phi$	$K = \dfrac{a_S}{C_S^2}\cos^3\phi$
	$\varepsilon_{lm} = \dfrac{V_S}{2C_S}$ for $\phi = 45°$	$\varepsilon_{nm} = \dfrac{V_S}{2C_S}$ for $\phi = 45°$	$\gamma_m = \dfrac{V_S}{C_S}$ for $\phi = 0°$	$K_m = \dfrac{a_S}{C_S^2}$ for $\phi = 0°$
Rayleigh wave Compressional component	$\varepsilon_l = \dfrac{V_{RP}}{C_R}\cos^2\phi$	$\varepsilon_n = \dfrac{V_{RP}}{C_R}\sin^2\phi$	$\gamma = \dfrac{V_{RP}}{C_R}\sin\phi\cos\phi$	$K = \dfrac{a_{RP}}{C_R^2}\sin\phi\cos^2\phi$
	$\varepsilon_{lm} = \dfrac{V_{RP}}{C_R}$ for $\phi = 0°$	$\varepsilon_{nm} = \dfrac{V_{RP}}{C_R}$ for $\phi = 90$	$\gamma_m = \dfrac{V_P}{2C_R}$ for $\phi = 45°$	$K_m = 0.385\dfrac{a_{RP}}{C_R^2}$ for $\phi = 35°16'$
Shear component		$\varepsilon_n = \dfrac{V_{RS}}{C_R}\sin\phi$	$\gamma = \dfrac{V_{RP}}{C_R}\cos\phi$	$K = \dfrac{a_{RS}}{C_R^2}\cos^2\phi$
		$\varepsilon_{nm} = \dfrac{V_{RS}}{C_R}$ for $\phi = 90°$	$\gamma_m = \dfrac{V_{RS}}{C_R}$ for $\phi = 0°$	$K_m = \dfrac{a_{RS}}{C_R^2}$ for $\phi = 0°$

The Poisson's ratio and dynamic modulus of a soil deposit can be computed from measured P- and S-wave propagation velocities in an elastic medium: $v_m = \dfrac{1}{2}\dfrac{(C_p/C_s)^2 - 2}{(C_p/C_s)^2 - 1}$ or $C_P = \sqrt{\dfrac{2(1 - v_m)}{(1 - v_m)}}C_S$; $E_m = \rho C_P^2 \dfrac{(1 + v_m)(1 - 2v_m)}{(1 - v_m)}$; and $G_m = \rho C_S^2$, respectively.

Table 6
Seismic racking design approaches (after Wang, 1993)

Approaches	Advantages	Disadvantages	Applicability
Dynamic earth pressure methods	1. Used with reasonable results in the past 2. Require minimal parameters and computation error 3. Serve as additional safety measures against seismic loading	1. Lack of rigorous theoretical basis 2. Resulting in excessive racking deformations for tunnels with significant burial 3. Use limited to certain types of ground properties	For tunnels with minimal soil cover thickness
Free-field racking deformation method	1. Conservative for tunnel structure stiffer than ground 2. Comparatively easy to formulate 3. Used with reasonable results in the past	1. Non-conservative for tunnel structure more flexible than ground 2. Overly conservative for tunnel structures significantly stiffer than ground 3. Less precision with highly variable ground conditions	For tunnel structures with equal stiffness to ground
Soil–structure interaction finite-element analysis	1. Best representation of soil–structure system 2. Best accuracy in determining structure response 3. Capable of solving problems with complicated tunnel geometry and ground conditions	1. Requires complex and time consuming computer analysis 2. Uncertainty of design seismic input parameters may be several times the uncertainty of the analysis	All conditions
Simplified frame analysis model	1. Good approximation of soil–structure interaction 2. Comparatively easy to formulate 3. Reasonable accuracy in determining structure response	1. Less precision with highly variable ground	All conditions except for compacted subsurface ground profiles

Ground shear distortions can be defined in two ways, as shown in Fig. 11. In the non-perforated ground, the maximum diametric strain is a function of maximum free-field shear strain only:

$$\frac{\Delta d}{d} = \pm \frac{\gamma_{max}}{2}. \tag{8}$$

The diametric strain in a perforated ground is further related to the Poisson's ratio of the medium:

$$\frac{\Delta d}{d} = \pm 2\gamma_{max}(1 - \nu_m). \tag{9}$$

Both of these equations assume the absence of the lining, therefore ignoring tunnel–ground interaction. In the free-field, the perforated ground would yield a much greater distortion than the non-perforated,

sometimes by a factor of two or three. This provides a reasonable distortion criterion for a lining with little stiffness relative to the surrounding soil, while the
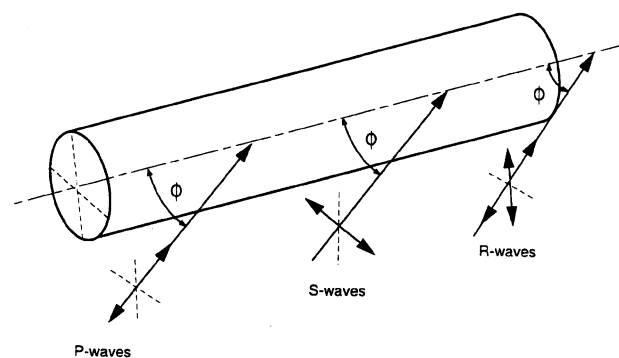

Fig. 10. Seismic waves causing longitudinal axial and bending strains (Power et al., 1996).
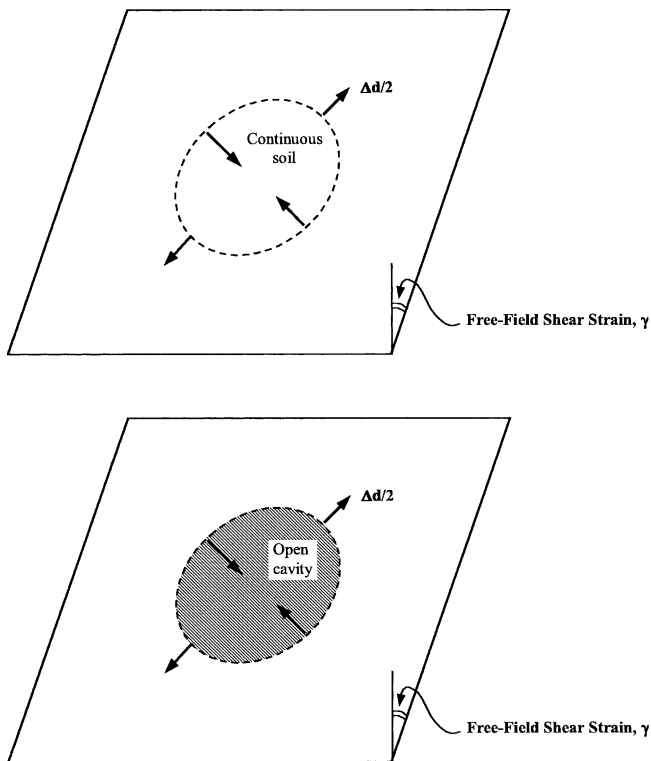
Fig. 11. Free-field shear distortion of perforated and non-perforated ground, circular shape (after Wang, 1993).

non-perforated deformation equation will be appropriate when the lining stiffness is equal to that of the medium. A lining with large relative stiffness should experience distortions even less than those given by Eq. (8) (Wang, 1993).

7.1.3. Racking deformations of rectangular tunnels

When subjected to shear distortions during an earthquake, a rectangular box structure will undergo transverse racking deformations (Fig. 12). The racking deformations can be computed from shear strains in the soil such as those given in Table 5.

7.1.4. Numerical analysis

Numerical analysis may be necessary to estimate the free-field shear distortions, particularly if the site stratigraphy is variable. Many computer programs are available for such analyses such as 1-D wave propagation programs listed in Section 4.5, as well as FLUSH (Lysmer et al., 1975), and LINOS (Bardet, 1991). Most programs model the site geology as a horizontally layered system and derive a solution using one-dimensional wave propagation theory (Schnabel et al., 1972). Navarro (1992) presents numerical computations for ground deformations and pressures as a result of body (shear and compression) wave as well as surface (Rayleigh and Love) waves. The resulting free-field shear distortion can then be expressed as a shear strain distribution or shear deformation profile with depth.

7.1.5. Applicability of free field deformation approach

The free-field racking deformation method has been used on many significant projects, including the San Francisco BART stations and tunnels (Kuesel, 1969) and the Los Angeles Metro (Monsees and Merritt, 1991). Kuesel found that, in most cases, if a structure can absorb free-field soil distortions elastically, no special seismic provisions are necessary. Monsees and Merritt (1991) further specified that joints strained into plastic hinges can be allowed under the Maximum Design Earthquake (MDE), provided no plastic hinge combinations are formed that could lead to a collapse mechanism, as shown in Fig. 13.

The free-field deformation method is a simple and effective design tool when seismically-induced ground distortions are small (i.e. low shaking intensity, very stiff ground, or the structure is flexible compared to the surrounding medium). However, in many cases, especially in soft soils, the method gives overly conservative designs because free-field ground distortions in soft soils are generally large. For example, rectangular box structures in soft soils are typically designed with stiff configurations to resist static loads and are therefore,
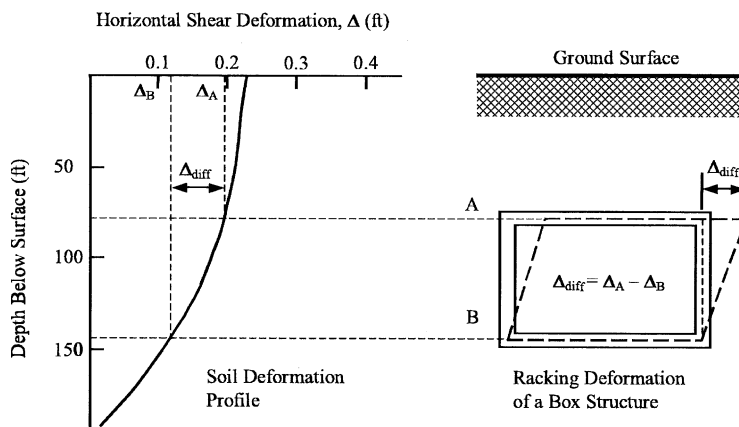

Fig. 12. Typical free-field racking deformation imposed on a buried rectangular frame (after Wang, 1993).
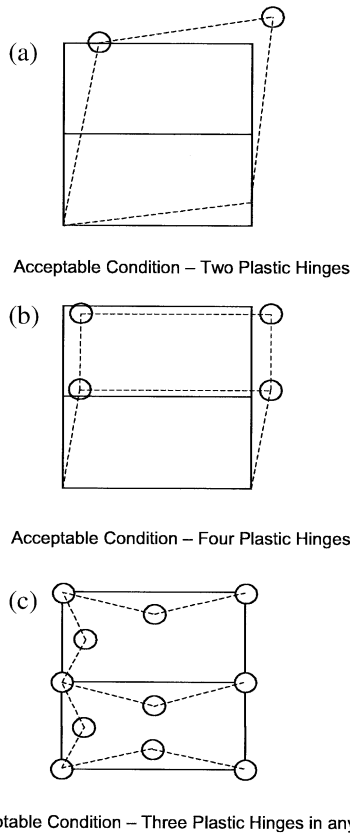
Fig. 13. Structure stability for buried rectangular frames (after Wang, 1993).

less tolerant to racking distortions (Hwang and Lysmer, 1981; TARTS, 1989). Soil–structure interaction effects have to be included for the design of such structures (Wang, 1993). A comparison of the free field deformation approach with other methods for seismic racking design is given in Table 6.

7.2. Soil structure interaction approach

The presence of an underground structure modifies the free field ground deformations. The following paragraphs describe procedures that model soil structure interaction.

7.2.1. Closed form elastic solutions for circular tunnels, axial force and moment

In this class of solutions the beam-on-elastic foundation approach is used to model (quasi-static) soil-structure interaction effects. The solutions ignore dynamic (inertial) interaction effects. Under seismic loading, the cross-section of a tunnel will experience axial bending and shear strains due to free field axial, curvature, and shear deformations. The maximum structural strains are (after St. John and Zahrah, 1987):

The maximum axial strain, caused by a 45° incident shear wave, Fig. 9, is:

$$\varepsilon_{\max}^{a} = \frac{\left(\frac{2\pi}{L}\right)A}{2 + \frac{E_l A_c}{K_a}\left(\frac{2\pi}{L}\right)^2} \le \frac{fL}{4E_l A_c} \qquad (10)$$

Where

L = wavelength of an ideal sinusoidal shear wave (see Eq. (15))
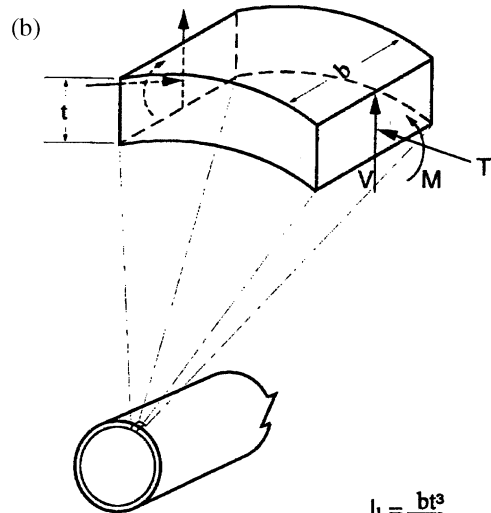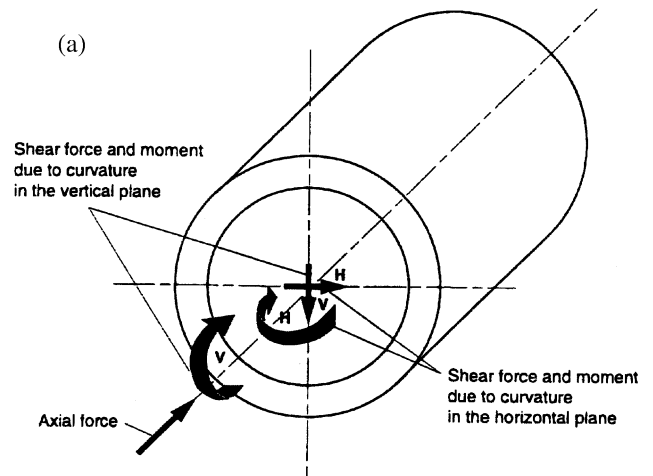
Fig. 14. Induced forces and moments caused by seismic waves (Power et al., 1996), (a) Induced forces and moments caused by waves propagating along tunnel axis, (b) Induced circumferential forces and moments caused by waves propagating perpendicular to tunnel axis.

K_a = longitudinal spring coefficient of medium (in force per unit deformation per unit length of tunnel, see Eq. (14))
A = free-field displacement response amplitude of an ideal sinusoidal shear wave (see Eqs. (17) and (18))
A_c = cross-sectional area of tunnel lining
E_l = elastic modulus of the tunnel lining
f = ultimate friction force (per unit length) between tunnel and surrounding soil

The forces and moments in the tunnel lining caused by seismic waves propagating along the tunnel axis are illustrated in Fig. 14a. The maximum frictional forces that can be developed between the lining and the surrounding soils limit the axial strain in the lining. This maximum frictional force, $(Q_{max})_f$, can be estimated as the ultimate frictional force per unit length times one-quarter the wave length, as shown in Eq. (10) (Sakurai and Takahashi, 1969).

The maximum bending strain, caused by a 0° incident shear wave, is:

$$\varepsilon_{max}^b = \frac{\left(\frac{2\pi}{L}\right)^2 A}{1 + \frac{E_l I_c}{K_t}\left(\frac{2\pi}{L}\right)^4} r \tag{11}$$

Where

I_c = moment of inertia of the tunnel section
K_t = transverse spring coefficient of the medium (in force per unit deformation per unit length of tunnel see Eq. (14))
r = radius of circular tunnel or half height of a rectangular tunnel

Since both the liner and the medium are assumed to be linear elastic, these strains may be superimposed. Since earthquake loading is cyclic, both extremes (positive and negative) must be evaluated. The maximum shear force acting on a tunnel cross-section can be written as a function of this maximum bending strain:

$$V_{max} = \frac{\left(\frac{2\pi}{L}\right)^3 E_l I_c A}{1 + \frac{E_l I_c}{K_t}\left(\frac{2\pi}{L}\right)^4} = \left(\frac{2\pi}{L}\right) M_{max}$$

$$= \left(\frac{2\pi}{L}\right)\left(\frac{E_l I_c \varepsilon_{max}^b}{r}\right) \tag{12}$$

A conservative estimate of the total axial strain and stress is obtained by combining the strains from the axial and bending forces (modified from Power et al., 1996):

$$\varepsilon^{ab} = \varepsilon_{max}^a + \varepsilon_{max}^b. \tag{13}$$

Again, these equations are necessary only for structures built in soft ground, as structures in rock or stiff soils can be designed using free-field deformations. It should be further noted that increasing the structural stiffness and the strength capacity of the tunnel may not result in reduced forces — the structure may actually attract more force. Instead, a more flexible configuration with adequate ductile reinforcement or flexible joints may be more efficient (Wang, 1993).

7.2.1.1. Spring coefficients. Other expressions of maximum sectional forces exist in the literature (SFBART, 1960; Kuribayashi et al., 1974; JSCE, 1975), with the major differences involving the maximization of forces and displacements with respect to wavelength. JSCE (1975) suggests substituting the values of wavelength that will maximize the stresses back into each respective equation to yield maximum sectional forces. St. John and Zahrah (1987) suggest a maximization method similar to the JSCE (1975) approach, except that the spring coefficients K_a and K_t are considered functions of the incident wavelength:

$$K_t = K_a = \frac{16\pi G_m(1 - \nu_m)}{(3 - 4\nu_m)}\frac{d}{L} \tag{14}$$

where G_m, ν_m = shear modulus and Poisson's ratio of the medium, d = diameter of circular tunnel (or height of rectangular structure).

These spring constants represent (1) the ratio of pressure between the tunnel and the medium, and (2) the reduced displacement of the medium when the tunnel is present. The springs differ from those of a conventional beam analysis on an elastic foundation. Not only must the coefficients be representative of the dynamic modulus of the ground, but the derivation of these constants must consider the fact that the seismic loading is alternately positive and negative due to the assumed sinusoidal wave (Wang, 1993). When using these equations to calculate the forces and moments for tunnels located at shallow depths, the soil spring resistance values are limited by the depth of cover and lateral passive soil resistance.

7.2.1.2. Idealized sinusoidal free field wave parameters for use in soil−structure interaction analysis. Matsubara et al. (1995) provide a discussion of input wavelengths for underground structure design. The incident wavelength of a ground motion may be estimated as:
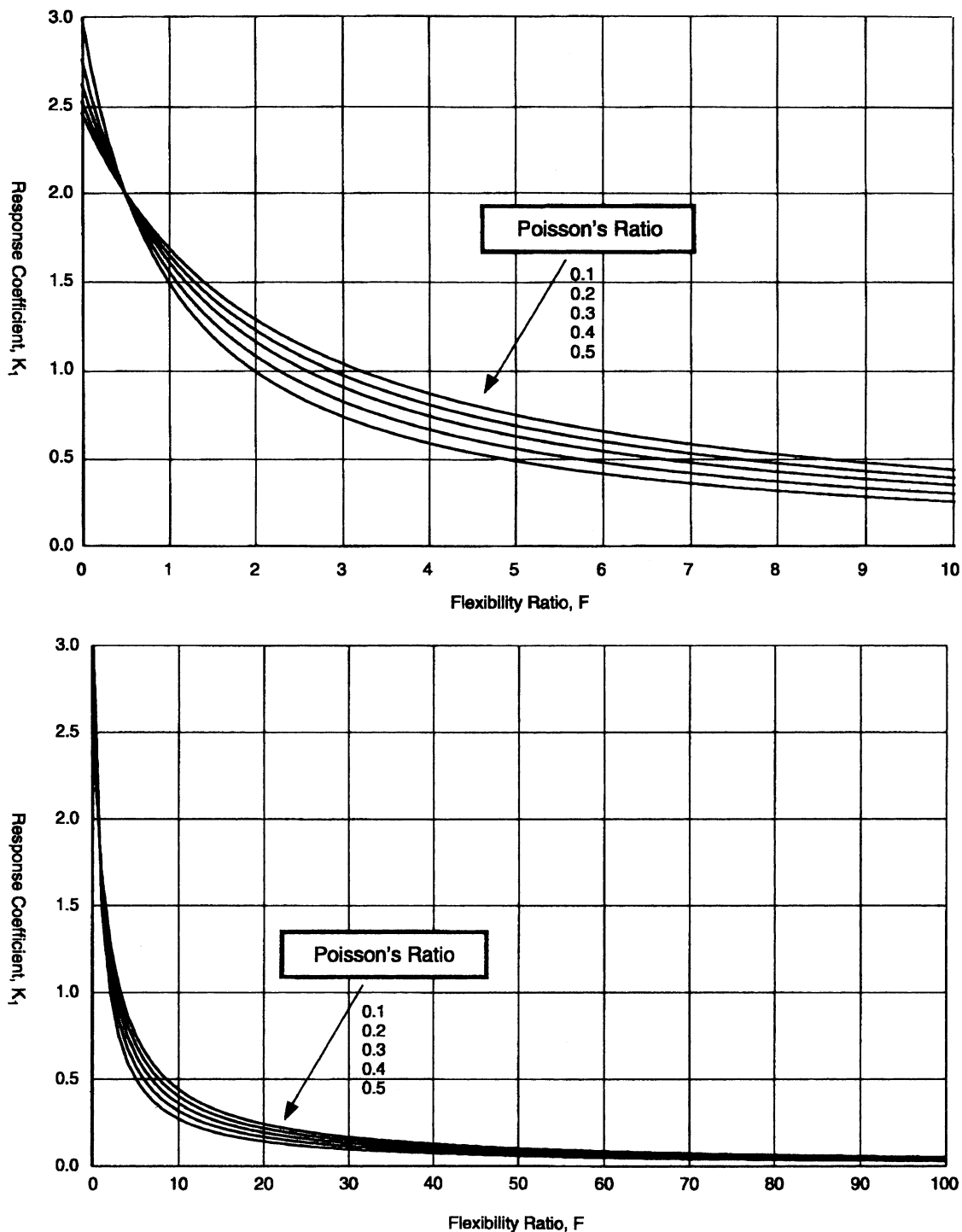
$$L = T \cdot C_s \tag{15}$$

Fig. 15. Lining response coefficient vs. flexibility ratio, full-slip interface, and circular tunnel (Wang, 1993).

where T is the predominant natural period of a shear wave in the soil deposit, the natural period of the site itself, or the period at which maximum displacements occur (Dobry et al., 1976; Power et al., 1996).

Idriss and Seed (1968) recommend that:

$$T = \frac{4h}{C_S}, \quad h \text{ is the thickness of the soil deposit} \qquad (16)$$

if ground motion can be attributed primarily to shear waves and the medium is assumed to consist of a uniform soft soil layer overlying a stiff layer (St. John and Zahrah, 1987).

The ground displacement response amplitude, A, represents the spatial variations of ground motions along a horizontal alignment and should be derived by site-specific subsurface conditions. Generally, the dis-

placement amplitude increases with increasing wavelength (SFBART, 1960). Assuming a sinusoidal wave with a displacement amplitude A and a wavelength L, A can be calculated from the following equations:

For free-field axial strains:

$$\frac{2\pi A}{L} = \frac{V_s}{C_S} \sin\phi \cos\phi. \tag{17}$$

For free-field bending strains:

$$\frac{4\pi^2 A}{L^2} = \frac{a_s}{C_S} \cos^3\phi. \tag{18}$$

7.2.2. Ovaling deformations of circular tunnels

In early studies of racking deformations, Peck et al. (1972), based on earlier work by Burns and Richard (1964) and Hoeg (1968), proposed closed-form solutions in terms of thrusts, bending moments, and displacements under external loading conditions. The response of a tunnel lining is a function of the compressibility and flexibility ratios of the structure, and the in-situ overburden pressure ($\gamma_t h$) and at-rest coefficient of earth pressure (K_0) of the soil. To adapt to seismic loadings caused by shear waves, the free-field shear stress replaces the in-situ overburden pressure and the at-rest coefficient of earth pressure is assigned a value of (-1) to simulate the field simple shear condition. The shear stress can be further expressed as a function of shear strain.

The stiffness of a tunnel relative to the surrounding ground is quantified by the compressibility and flexibility ratios (C and F), which are measures of the extensional stiffness and the flexural stiffness (resistance to ovaling), respectively, of the medium relative to the lining (Merritt et al., 1985):

$$C = \frac{E_m(1 - v_l^2)r}{E_l t(1 + v_m)(1 - 2v_m)} \tag{19}$$

$$F = \frac{E_m(1 - v_l^2)R^3}{6E_l I(1 + v_m)} \tag{20}$$

where E_m = modulus of elasticity of the medium, I = moment of inertia of the tunnel lining (per unit width) for circular lining R, and t = radius and thickness of the tunnel lining.

Assuming full-slip conditions, without normal separation and therefore, no tangential shear force, the diametric strain, the maximum thrust, and bending moment can be expressed as (Wang, 1993):

$$\frac{\Delta d}{d} = \pm \frac{1}{3} K_1 F \gamma_{max} \tag{21}$$

$$T_{max} = \pm \frac{1}{6} K_1 \frac{E_m}{(1 + v_m)} r \gamma_{max} \tag{22}$$

$$M_{max} = \pm \frac{1}{6} K_1 \frac{E_m}{(1 + v_m)} r^2 \gamma_{max} \tag{23}$$

where

$$K_1 = \frac{12(1 - v_m)}{2F + 5 - 6v_m}. \tag{24}$$

These forces and moments are illustrated in Fig. 14b. The relationship between the full-slip lining response coefficient (K_1) and flexibility ratio is shown in Fig. 15.

According to various studies, slip at the interface is only possible for tunnels in soft soils or cases of severe seismic loading intensity. For most tunnels, the interface condition is between full-slip and no-slip, so both cases should be investigated for critical lining forces and deformations. However, full-slip assumptions under simple shear may cause significant underestimation of the maximum thrust, so it has been recommended that the no-slip assumption of complete soil continuity be made in assessing the lining thrust response (Hoeg, 1968; Schwartz and Einstein, 1980):

$$T_{max} = \pm K_2 \tau_{max} r = \pm K_2 \frac{E_m}{2(1 + v_m)} r \gamma_{max} \tag{25}$$

where

$$K_2 = 1 + \frac{F[(1 - 2v_m) - (1 - 2v_m)C] - \frac{1}{2}(1 - 2v_m)^2 + 2}{F[(3 - 2v_m) + (1 - 2v_m)C] + C\left[\frac{5}{2} - 8v_m + 6v_m^2\right] + 6 - 8v_m}. \tag{26}$$

As Fig. 16 shows, seismically-induced thrusts increase with decreasing compressibility and flexibility ratios when the Poisson's ratio of the surrounding ground is less than 0.5. As Poisson's ratio approaches 0.5 (i.e. saturated undrained clay), the thrust response is independent of compressibility because the soil is considered incompressible (Wang, 1993).

The normalized lining deflection provides an indication of the importance of the flexibility ratio in lining response, and is defined as (Wang, 1993):

$$\frac{\Delta d_{lining}}{\Delta d_{free-field}} = \frac{2}{3} K_1 F. \tag{27}$$

According to this equation and Fig. 17, a tunnel lining will deform less than the free field when the flexibility ratio is less than one (i.e. stiff lining in soft

soil). As the flexibility ratio increases, the lining deflects more than the free field and may reach an upper limit equal to the perforated ground deformations. This condition continues as the flexibility ratio becomes infinitely large (i.e. perfectly flexible lining).

Penzien and Wu (1998) developed similar closed-form elastic solutions for thrust, shear, and moment in the tunnel lining due to racking deformations. Penzien (2000) provided an analytical procedure for evaluating racking deformations of rectangular and circular tunnels that supplemented the previous publication.

In order to estimate the distortion of the structure, a lining-soil racking ratio is defined as:

$$R = \frac{\Delta_{\text{structure}}}{\Delta_{\text{free-field}}}. \tag{28}$$

In the case of circular tunnel, R is the ratio of lining diametric deflection and free-field diametric deflection. Assuming full slip condition, solutions for thrust, moment, and shear in circular tunnel linings caused by soil-structure interaction during a seismic event are expressed as (Penzien, 2000):

$$\pm\Delta d_{\text{lining}}^n = \pm R^n \Delta d_{\text{free-field}} \tag{29}$$

$$T(\theta) = -\frac{12 E_l I \Delta d_{\text{lining}}^n}{d^3(1-v_l^2)}\cos2\left(\theta + \frac{\pi}{4}\right) \tag{30}$$

$$M(\theta) = -\frac{6 E_l I \Delta d_{\text{lining}}^n}{d^2(1-v_l^2)}\cos2\left(\theta + \frac{\pi}{4}\right) \tag{31}$$

$$V(\theta) = -\frac{24 E_l I \Delta d_{\text{lining}}^n}{d^3(1-v_l^2)}\sin2\left(\theta + \frac{\pi}{4}\right) \tag{32}$$

The lining-soil racking ratio under normal loading only is defined as:

$$R^n = \pm\frac{4(1-v_m)}{(\alpha^n + 1)} \tag{33}$$

$$\alpha^n = \frac{12 E_l I(5-6v_m)}{d^3 G_m(1-v_l^2)}. \tag{34}$$

The sign convention for the above force components in circular lining is shown in Fig. 18. In the case of no slip condition, the formulations are presented as:

$$\pm\Delta d_{\text{lining}} = \pm R\Delta d_{\text{free-field}} \tag{35}$$

$$T(\theta) = -\frac{24 E_l I \Delta d_{\text{lining}}}{d^3(1-v_l^2)}\cos2\left(\theta + \frac{\pi}{4}\right) \tag{36}$$
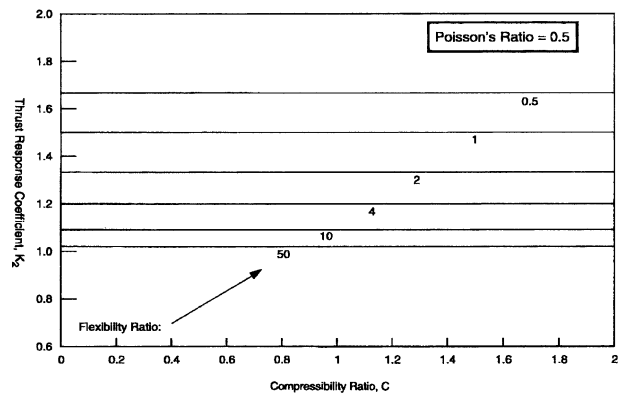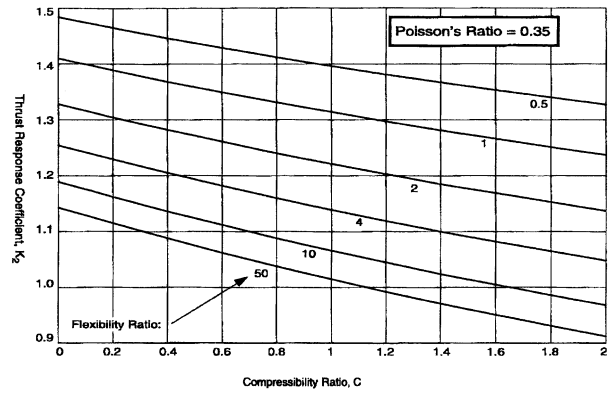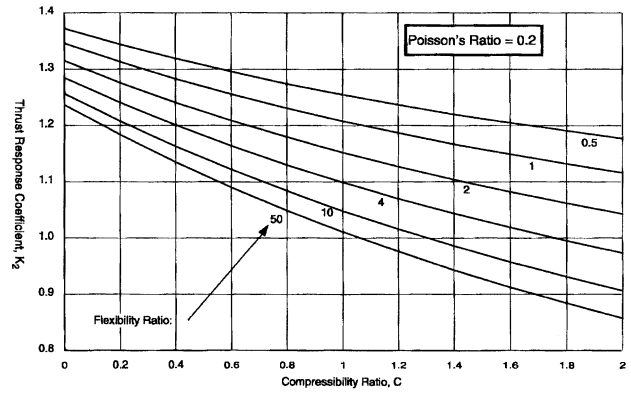

Fig. 16. Lining (thrust) response coefficient vs. compressibility ratio, no-slip interface, and circular tunnel (Wang, 1993).

$$M(\theta) = -\frac{6 E_l I \Delta d_{\text{lining}}}{d^2(1-v_l^2)}\cos2\left(\theta + \frac{\pi}{4}\right) \tag{37}$$

$$V(\theta) = -\frac{24 E_l I \Delta d_{\text{lining}}}{d^3(1-v_l^2)}\sin2\left(\theta + \frac{\pi}{4}\right) \tag{38}$$

where

$$R = \pm\frac{4(1-v_m)}{(\alpha + 1)} \tag{39}$$

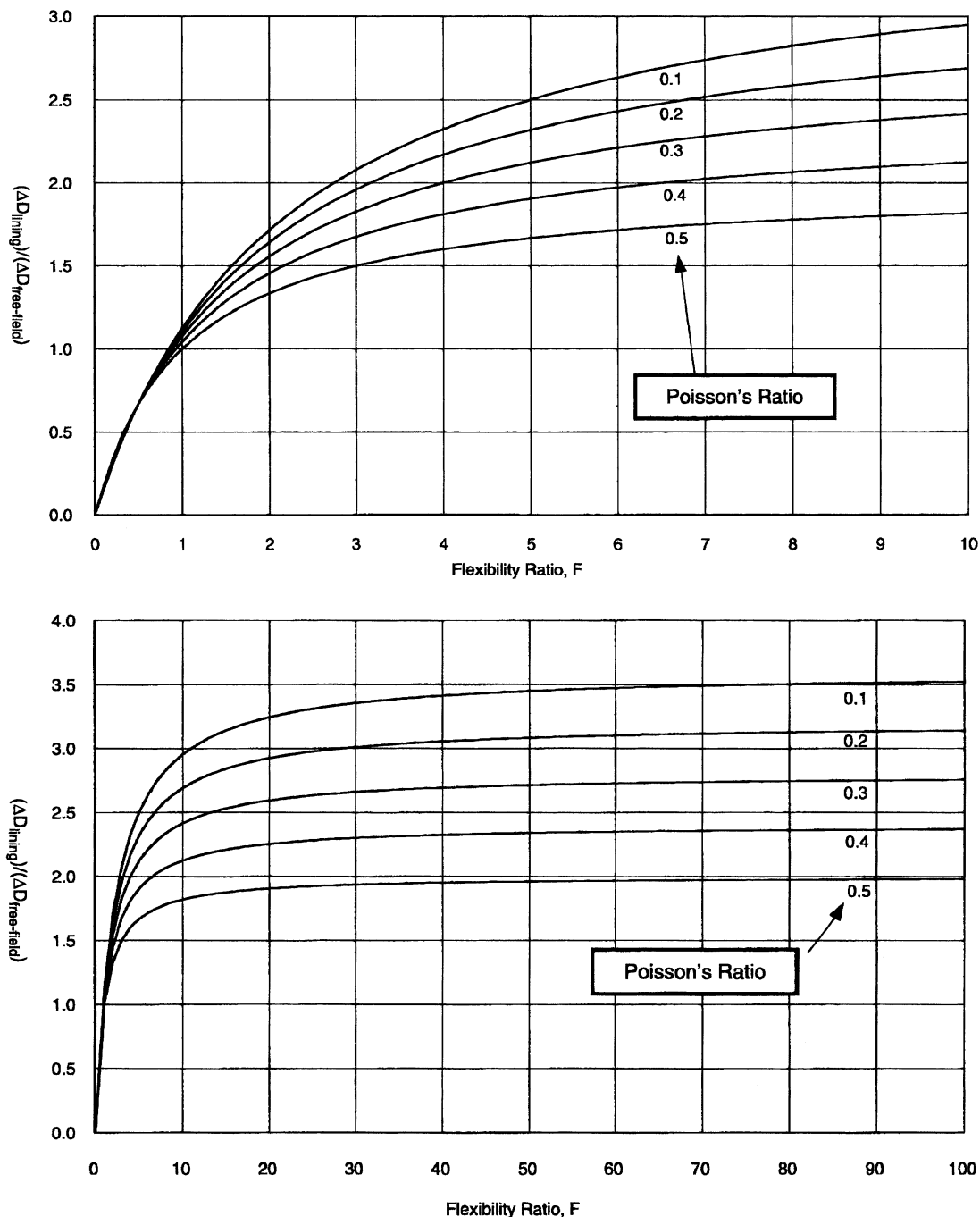$$\alpha = \frac{24 E_l I(3-4v_m)}{d^3 G_m(1-v_l^2)}. \tag{40}$$

Fig. 17. Normalized lining deflection vs. flexibility ratio, full slip interface, and circular lining (Wang, 1993).

The solutions of Penzien (2000) result in values of thrust and moment that are very close to those of Wang (1993) for full-slip condition. However, value of thrust obtained from Wang is much higher compared to the value given by Penzien in the case of no slip (see example 3 in Appendix B). This observation was also noted by Power et al. (1996). The reason for the difference is still under investigation.

7.2.3. Racking deformations of rectangular tunnels

Shallow transportation tunnels are usually box shaped

cut-and-cover method structures. These tunnels have seismic characteristics very different from circular tunnels. A box frame does not transmit static loads as efficiently as a circular lining, so the walls and slabs of the cut-and-cover frame need to be thicker, and therefore stiffer. The design of cut-and-cover structures requires careful consideration of soil-structure interaction effects because of this increased structural stiffness and the potential for larger ground deformations due to shallow burial. Seismic ground deformations tend to be greater at shallow depths for two reasons:

(1) the decreased stiffness of the surrounding soils due to lower overburden pressures; and (2) the site amplification effect. The soil backfill may also consist of compacted material with different properties from the in-situ soil, resulting in a different seismic response (Wang, 1993).

The structural rigidity of box structures significantly reduces computed strains, often making it overly conservative to design these structures based on free-field strains (Hwang and Lysmer, 1981). While closed-form solutions for tunnel-ground interaction problems are available for circular tunnels, they are not available for rectangular tunnels because of the highly variable geometric characteristics associated with these structures. For ease of design, simple and practical procedures have been developed to account for dynamic soil-structure interaction effects (Wang, 1993).

A number of factors contribute to the soil-structure interaction effect, including the relative stiffness between soil and structure, structure geometry, input earthquake motions, and tunnel embedment depth. The most important factor is the stiffness in simple shear of the soil relative to the structure that replaces it, the flexibility ratio (Wang, 1993).

Consider a rectangular soil element in a soil column under simple shear condition, as shown in Fig. 19. When subjected to simple shear stress the shear strain, or angular distortion, of the soil element is given by (Wang, 1993):

$$\gamma_s = \frac{\Delta}{H} = \frac{\tau}{G_m}. \tag{41}$$

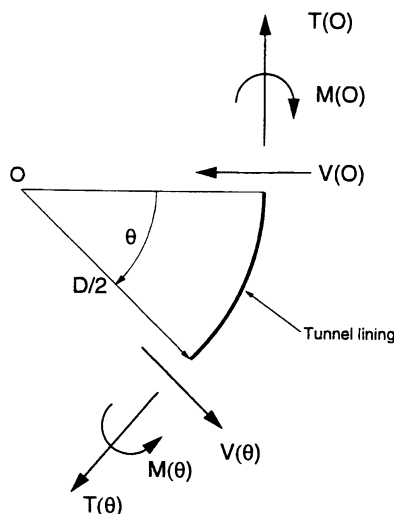After rearranging this equation, the shear or flexural

Fig. 18. Sign convention for force components in circular lining (after Penzien, 2000).
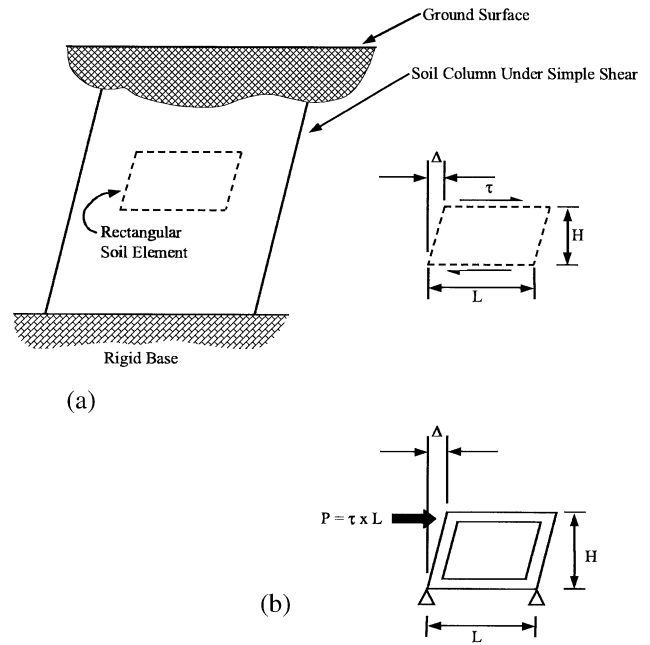

Fig. 19. Relative stiffness between soil and a rectangular frame (after Wang, 1993). (a) Flexural (shear) distortion of free-field soil medium. (b) Flexural (racking) distortion of a rectangular frame.

stiffness of the element can be written as the ratio of shear stress to a corresponding angular distortion:

$$\frac{\tau}{\gamma_s} = \frac{\tau}{\Delta/H} = G_m. \tag{42}$$

The applied shear stress can also be converted into a concentrated force, P, by multiplying it by the width of the structure (W), resulting in the following expression for the angular distortion (Wang, 1993):

$$\gamma_s = \frac{\Delta}{H} = \frac{P}{HS_1} = \frac{\tau W}{HS_1} \tag{43}$$

$$\frac{\tau}{\gamma_s} = \frac{\tau}{\Delta/H} = \frac{S_1 H}{W}. \tag{44}$$

where S_1 is the force required to cause a unit racking deflection of the structure. The flexibility ratio of the structure can then be calculated as previously discussed:

$$F = \frac{G_m W}{S_1 H}. \tag{45}$$

In these expressions, the unit racking stiffness is simply the reciprocal of the lateral racking deflection, $S_1 = 1/\Delta_1$, caused by a unit concentrated force.

For a rectangular frame with arbitrary configuration, the flexibility ratio can be determined by performing a simple frame analysis using a conventional frame anal-

ysis. For some simple one-barrel frames, the flexibility ratio can be calculated without a computer analysis. As an example, the flexibility ratio for a one-barrel frame with equal moment of inertia for roof and invert slabs (I_R) and moment of inertia for side walls (I_W) has been calculated as (Wang, 1993):

$$F = \frac{G_m}{24}\left(\frac{H^2 W}{EI_W} + \frac{HW^2}{EI_R}\right) \qquad (46)$$

where E = plane strain elastic modulus of frame.

For a one-barrel frame with roof slab moment of inertia (I_R), invert slab moment of inertia (I_I), and side wall moment of inertia (I_W), the flexibility ratio is:

$$F = \frac{G_m}{12}\left(\frac{HW^2}{EI_R}\Psi\right) \qquad (47)$$

where

$$\Psi = \frac{(1+a_2)(a_1 + 3a_2)^2 + (a_1 + a_2)(3a_2 + 1)^2}{(1 + a_1 + 6a_2)^2} \qquad (48)$$

$$a_1 = \left(\frac{I_R}{I_I}\right) \qquad (49)$$

$$a_2 = \left(\frac{I_R}{I_W}\right)\left(\frac{H}{W}\right). \qquad (50)$$

7.2.3.1. Structural racking and racking coefficient. For rectangular structure, the racking ratio (see Eq. (28)) defined as the normalized structure racking distortion with respect to the free-field ground distortion can be expressed as (Wang, 1993):

$$R = \frac{\Delta_{\text{structure}}}{\Delta_{\text{free-field}}} = \frac{\left(\dfrac{\Delta_{\text{structure}}}{H}\right)}{\left(\dfrac{\Delta_{\text{free-field}}}{H}\right)} = \frac{\gamma_{\text{structure}}}{\gamma_{\text{free-field}}} \qquad (51)$$

where γ = angular distortion, and Δ = lateral racking deformation.

The results of finite element analyses show that the relative stiffness between the soil and the structure that replaces it (i.e. flexibility ratio) has the most significant influence on the distortion of the structure due to racking deformations (Wang, 1993), for:

$F \rightarrow 0.0$ The structure is rigid, so it will not rack regardless of the distortion of the ground (i.e. the structure must take the entire load).

$F < 1.0$ The structure is considered stiff relative to the medium and will therefore deform less.

$F = 1.0$ The structure and medium have equal stiffness, so the structure will undergo approximately free-field distortions.

$F > 1.0$ The racking distortion of the structure is amplified relative to the free field, though not because of dynamic amplification. Instead, the distortion is amplified because the medium now has a cavity, providing lower shear stiffness than non-perforated ground in the free field.

$F \rightarrow \infty$ The structure has no stiffness, so it will undergo deformations identical to the perforated ground.

Analyses have also shown that for a given flexibility ratio, the normalized distortion of a rectangular tunnel is approximately 10% less than that of a circular tunnel (Fig. 20). This allows the response of a circular tunnel to be used as an upper bound for a rectangular structure with a similar flexibility ratio, and shows that conventional design practice (i.e. structures conform to the free-field deformations) for rectangular tunnels is too conservative for cases involving stiff structures in soft soil ($F < 1.0$). Conversely, designing a rectangular tunnel according to the free-field deformation method leads to an underestimation of the tunnel response when the flexibility ratio is greater than one. From a structural standpoint, this may not be of major concern because such flexibility ratios imply very stiff media and therefore, small free-field deformations. This condition may also imply a very flexible structure that can absorb greater distortions without distress (Wang, 1993).

The racking deformations can be applied to an underground structure using the equivalent static load method such as those shown in Fig. 21. For deeply buried rectangular structures, most of the racking is generally attributable to shear forces developed at the exterior surface of the roof. The loading may then be simplified as a concentrated force acting at the roof-wall connection (Fig. 21a). For shallow rectangular tunnels, the shear force developed at the soil/roof interface decreases with decreasing overburden. The predominant external force that causes structure racking may gradually shift from shear force at the soil/roof interface to normal earth pressures developed along the side walls, so a triangular pressure distribution is applied to the model (Fig. 21b). Generally, the triangular pressure distribution model provides a more critical value of the moment capacity of rectangular structures at bottom joints, while the concentrated force method gives a more critical moment response at the roof-wall joints (Wang, 1993).

The above discussion applies to tunnel structures in a homogeneous soil deposit. If the tunnel structure is at the interface between rigid and soft layers, the analysis has to account for the change in ground motion and shear deformation at the interface zone between the two soils.
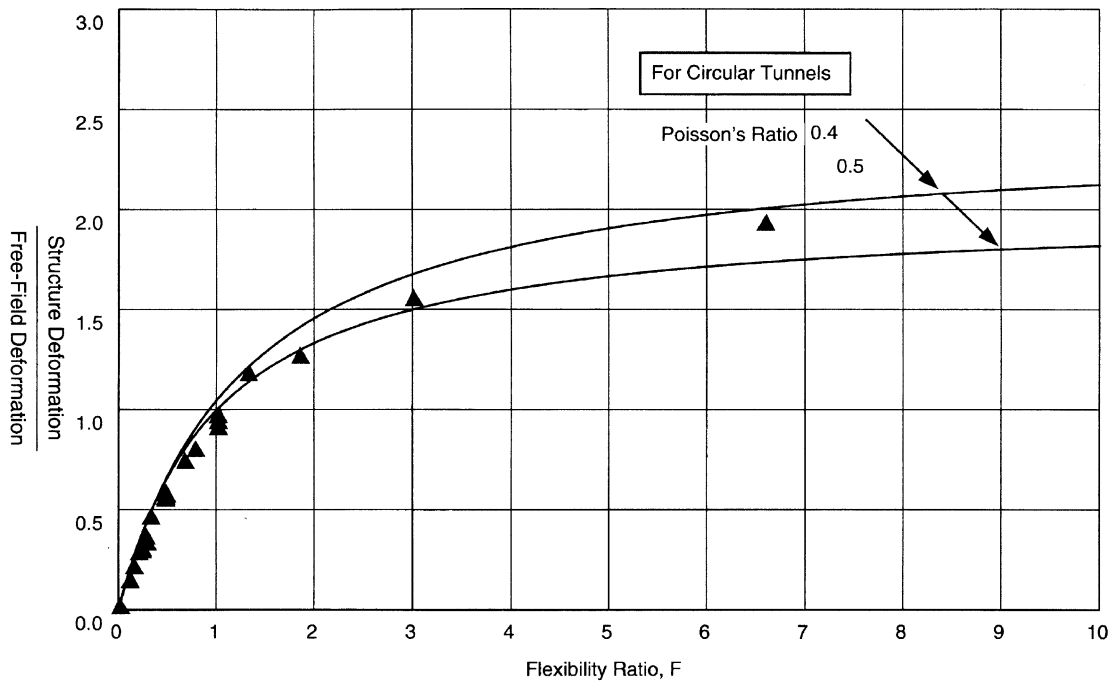
Filled Triangular Symbols: For Rectangular Tunnels
Solid Lines: For Circular Tunnels
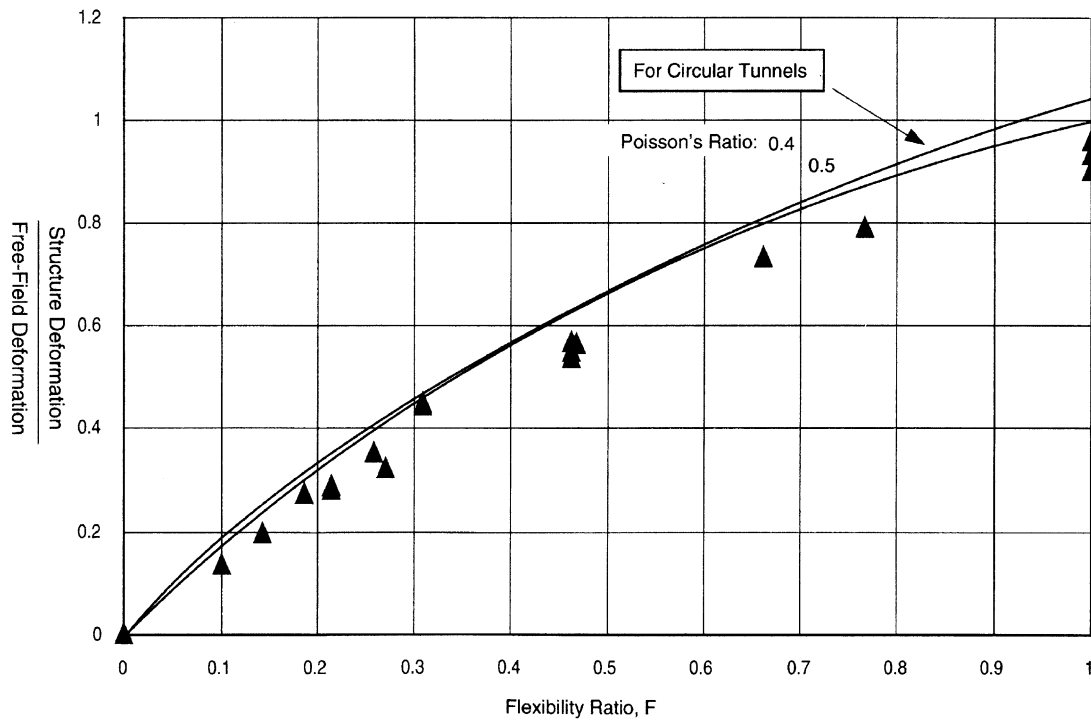
Filled Triangular Symbols: For Rectangular Tunnels
Solid Lines: For Circular Tunnels

Fig. 20. Normalized structure deflections, circular vs. rectangular tunnels (Wang, 1993).

7.2.3.2. Step-by-step design procedure. A simplified frame analysis can provide an adequate and reasonable design approach to the design of rectangular structures. The following is a step-by-step procedure for such an

analysis (based in part on Monsees and Merritt, 1988; Wang, 1993):

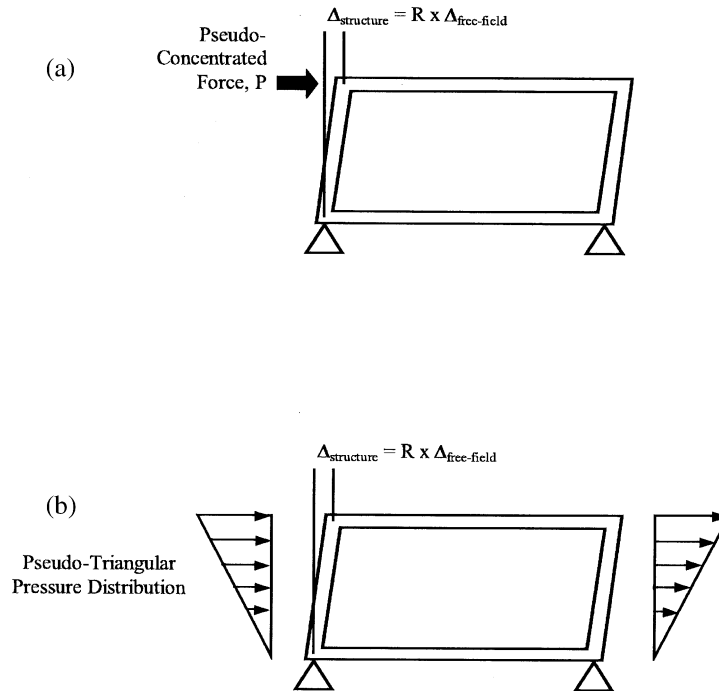1.   Base preliminary design of the structure and ini-

Fig. 21. Simplified frame analysis models (after Wang, 1993): (a) pseudo-concentrated force for deep tunnels; (b) pseudo-triangular pressure distribution for shallow tunnels.

tial sizes of members on static design and appropriate design requirements.

2. Estimate the free-field shear strains/deformations, $\Delta_{\text{free-field}}$, of the ground at the depth of interest using vertically propagating horizontal shear wave.

3. Determine the relative stiffness (i.e. the flexibility ratio) between the free-field medium and the structure.

4. Determine the racking coefficient, R as defined in Eq. (51), based on the flexibility ratio (e.g. Fig. 20).

5. Calculate the actual racking deformation of the structure as $\Delta_{\text{structure}} = R\Delta_{\text{free-field}}$.

6. Impose the seismically-induced racking deformation in a simple frame analysis.

7. Add the racking-induced internal member forces to the other loading components. If the permanent structure is designed for 'at-rest' earth pressures, no increase in pressures before or subsequent to an earthquake need to be considered. If the structure is designed for active earth pressures, both active and at-rest pressures should be used for dynamic loading.

8. If the results from (7) show that the structure has adequate capacity, the design is considered satisfactory. Otherwise, continue.

9. If the structure's flexural strength is exceeded in (7), check the members' rotational ductility. Special design provisions should be implemented if inelastic deformations result. For ODE, the resulting deformation should be kept within the elastic range. Small inelastic deformations may or may not be acceptable depending on the project-specific performance requirements. Evaluate possible mechanisms for MDE. Redistribution of moments in accordance with ACI 318 is acceptable and consideration of plastic hinges is acceptable. If plastic hinges develop the flexibility ratio has to be re-computed and the analysis restarted at step (3).

10. The structure should be redesigned if the strength and ductility requirements are not met, and/or the resulting inelastic deformations exceed allowable levels (depending upon the performance goals of the structure).

11. Modify the sizes of structural elements as necessary. The design is complete for MDE if ultimate conditions in the context of plastic design are not exceeded at any point for the reinforcement selected in initial static design. Reinforcing steel percentages may need to be adjusted to avoid brittle behavior. Under static or pseudo-static loads, the maximum usable compressive concrete strain is 0.004 for flexure and 0.002 for axial loading.

In addition to racking deformations the design of cut and cover structure should also account for loads due to vertical accelerations and for longitudinal strain resulting from frictional soil drag. Vertical seismic forces exerted on the roof of a cut-and-cover tunnel
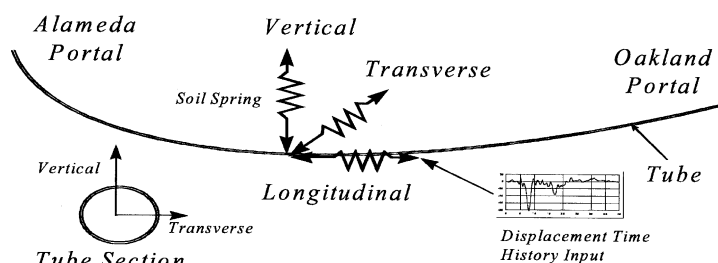
Fig. 22. Simplified three-dimensional model for analysis of the global response of an immersed tube tunnel (Hashash et al. 1998).

structure may be estimated by multiplying the estimated peak vertical ground acceleration by the backfill mass.

7.2.4. Dynamic earth pressure

Dynamic earth pressures on cut-and-cover tunnel structures take the form of complex shear and normal stress distributions along the exterior surfaces of the structure. Accurately quantifying these external loads requires rigorous dynamic soil-structure analyses. Whitman (1990) presents a state-of-the-art review of dynamic earth pressures.

Dynamic earth pressure methods typically assume earthquake loads to be caused by the inertial force of the surrounding soils. One procedure commonly used for determining the increase in lateral earth pressure is the Mononobe–Okabe method, as suggested by Seed and Whitman (1970), and the Japanese Society of Civil Engineers (JSCE, 1975). This method calculates the dynamic earth pressure by relating it to the soil properties and a determined seismic coefficient. The Mononobe–Okabe method was originally developed for aboveground earth retaining walls, and assumes the wall structure to move and/or tilt sufficiently for a yielding active earth wedge to form behind the wall. However, a buried rectangular structural frame will move together with the ground, making the formation of a yielding active wedge difficult.

For rectangular cross-sections under plane strain conditions, the Mononobe–Okabe method leads to unrealistic results and is not recommended for typical tunnel sections. In general, the deeper the tunnel embedment, the less reliable the estimated seismic lateral earth pressures because it becomes increasingly important to account for variations in seismic ground motions with depth. Displacement/deformation controlled procedure, as outlined in previous sections, should be used for tunnels.

7.2.5. Numerical methods

The complex nature of the seismic soil–structure interaction problem for underground structures may require the use of numerical methods. This is especially true for cut-and-cover structures because of their greater vulnerability to seismic damage, and mined tunnels with non-circular shapes or non-uniform properties of circular linings that preclude the use of simple closed-form solutions.

Numerical analysis methods for underground structures include lumped mass/stiffness methods and finite element/difference methods. For analyzing axial and bending deformations, it is most appropriate to utilize three-dimensional models. In the lumped mass method, the tunnel is divided into a number of segments (masses/stiffness), which are connected by springs representing the axial, shear, and bending stiffness of the tunnel. The soil reactions are represented by horizontal, vertical, and axial springs (Hashash et al., 1998, Fig. 22), and the analysis is conducted as an equivalent static analysis. Free-field displacement time histories are first computed at selected locations along the tunnel length. The time histories must include the effects of wave passage/phase shift as well as incoherence (Section 4.4.3). The computed free-field displacement time histories are then applied, in a quasi-static analysis, at the ends of the springs representing the soil-tunnel interaction. If a dynamic, time-history analysis is desired appropriate damping factors have to be incorporated into the springs and the structure.

In finite difference or finite element models, the tunnel is discretized spatially, while the surrounding geologic medium is either discretized or represented by soil springs. Computer codes available for these models include FLAC[3D] (Itasca, 1995), SASSI (Lysmer et al., 1991), FLUSH (Lysmer et al., 1975), ANSYS-III (Oughourlian and Powell, 1982), ABAQUS (Hibbitt et al., 1999), and others. Two-dimensional and three-dimensional finite element and finite difference models may be used to analyze the cross section of a bored tunnel or cut-and-cover tunnel (Figs. 23 and 24). In Fig. 24, the finite element method is used to check areas of structure that experience plastic behavior.

In cases where movement along weak planes in the geologic media (shear zones, bedding planes, joints) may potentially cause local stress concentrations and failures in the tunnel, analyses using discrete element models may be considered. In these models, the soil/rock mass is modeled as an assemblage of distinct blocks, which may in turn be modeled as either rigid or deformable materials, each behaving according to a
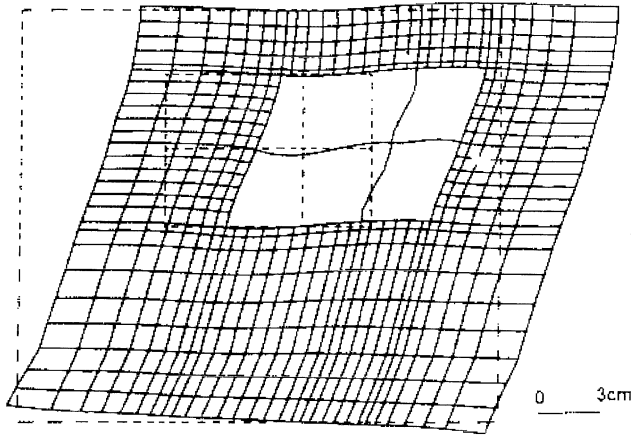
Fig. 23. Distribution of maximum displacement in a cut and cover structure (Matsuda et al., 1996).

prescribed constitutive relationship. The relative movements of the blocks along weak planes are modeled using force-displacement relationships in both normal and shear directions (Power et al., 1996). UDEC (Itasca, 1992) and DDA (Shi, 1989) are two computer codes for this type of analysis.

Gomez-Masso and Attalla (1984) performed an extensive study comparing detailed finite element analyses with several simplified tunnel models and found
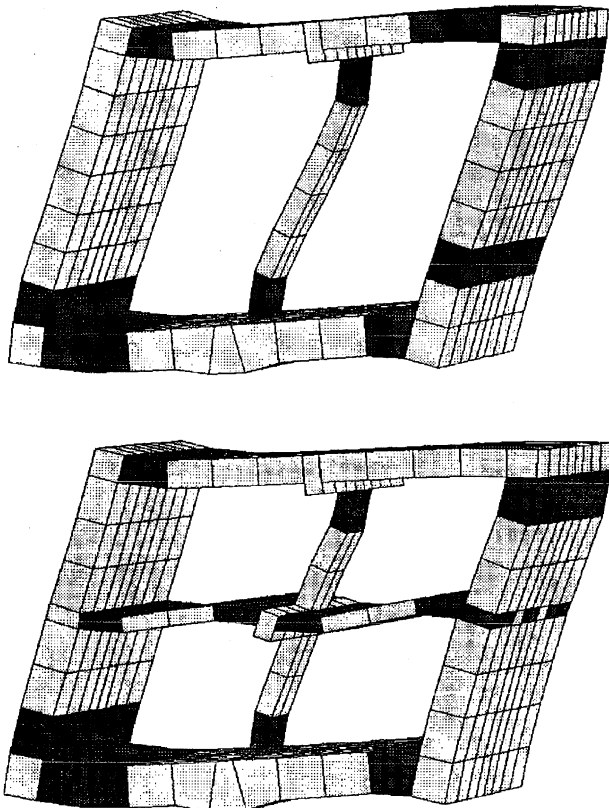

Fig. 24. Deformed cut-and-cover structures. Darkened elements experience plastic behavior (Sweet, 1997).

that, with few exceptions, simplified methods tend to be very conservative. One reason for this finding is that the simplified methods they used fail to consider structure-to-structure interaction effects through the soil, which are important in this case.

The results of non-linear analyses of the Los Angeles Metro system (Sweet, 1997) displayed structural racking greater than the free-field, though previous linear analyses showed smaller racking. This supports the assertion that both the non-linear structural behavior and the frequency content of the free-field environment contribute to the structural-racking behavior. Manoogian (1998) shows through a parametric study that the ground motion may be significantly amplified due to the presence underground structures. However, the study assumes the soil medium to be an elastic half-space and the tunnel lining to be elastic, limiting their applicability given the significant non-linearity associated with the soil behavior and associated strong motion events.

The ability of numerical analyses to improve on closed form solutions lies in the uncertainty of input data. If there is significant uncertainty in the input, refined analyses may not be of much value (St. John and Zahrah, 1987). A similar cautionary remark was made by Kuesel (1969) noting that 'mathematical elaboration of this complex subject does not necessarily lead to increased understanding of its nature', and places high priority on developing 'a picture of the action of underground structures subjected to earthquakes, and to put reasonable bounds on the problem'.

8. Special seismic design issues

8.1. Tunnel joints at portals and stations

Underground structures often have abrupt changes in structural stiffness or ground conditions. Some examples include: (1) connections between tunnels and buildings or transit stations; (2) junctions of tunnels; (3) traversals between distinct geologic media of varying stiffness; and (4) local restraints on tunnels from movements of any type ('hard spots'). At these locations, stiffness differences may subject the structure to differential movements and generate stress concentrations. The most common solution to these interface problems involves the use of flexible joints.

For cases where the tunnel structure is rigidly connected to a portal building or a station, Yeh (1974) and Hetenyi (1976) developed a solution to estimate the additional moment and shear stresses induced at a tunnel-station interface due to the differential transverse deflections.

The design of seismic joints must begin with a de-

termination of the required and allowable differential movements in both the longitudinal and transverse directions and relative rotation. The joint must also be designed to support the static and dynamic earth and water loads expected before and during an earthquake, and must remain watertight. The differential movements can be computed using closed form solutions or numerical methods. In the case of the San Francisco Trans Bay Tube and Ventilation Building, these movements were calculated to be ± 37 and ± 150 mm in the vertical and longitudinal directions, respectively. Details of the joint used in the SF BART project are discussed in Douglas and Warshaw (1971).

For the Alameda Tubes retrofit design (Schmidt et al., 1998; Hashash et al., 1998), two separate dynamic soil structure interaction analyses were performed for the portal structure and the running tunnel. The tunnel and the portal building were assumed to move independent of one another. A displacement time history was computed at the portal building and at the end of the tunnel where it would join the portal building. The portal building-tunnel joint would have to accommodate the differential displacement that is computed as the difference between the two displacement time histories. The analyses showed that, as in the case for the BART Trans Bay tubes, the longitudinal differential displacements were significantly larger than the transverse displacements.

Very large forces and moments will be generated if a continuous design is used (Okamoto et al., 1973; Hashash et al., 1998). A flexible joint is recommended to permit differential movement between the tunnel and the portal structure.

In any soil-to-rock transition zone, Kuesel (1969) recommends that a tunnel structure should not be cast directly against any rock or any rock ridge within the soil. A tunnel should be provided with at least 600 mm of over-excavation filled with soil or aggregate backfill to prevent a hard point during seismic activity. However, this may not always be possible with bored tunnels, and flexible lining would be installed in such zones.

Tunnel portal and vent structures differ from other underground structures in that part of the structure is above ground. The seismic design of these structures will have to account for inertial effects such as described by Kiyomiya (1995) and Iwasaki (1984). The design will also have to account for potential of pounding between the structure and the connecting tunnel due to differential movement. It is preferable that the portal or vent structure be isolated from the tunnel structure through the use of flexible joints.

8.2. Tunnel segment connection design

The analysis methods for tunnel racking presented in Section 7 assume that the cross section of the tunnel lining is continuous. When a tunnel is excavated using a tunneling machine, the tunnel lining is usually erected in segments that are secured together by bolts. The segment joint connection must be designed to accommodate anticipated ground deformations. The designer may choose to keep the joint behavior within the elastic range or, if inelastic response is anticipated by a more detailed model of the joint, must consider lining ground interaction. Takada and Abdel-Aziz (1997) present such analysis, showing that under high levels of ground shaking, plastic extensions of the segment joints can occur and lead to possible water leakage after a seismic event.

8.3. Seismic retrofit of existing facilities

Retrofitting strategies for ground shaking-induced failure depend on the damage mode of the structure. If there is concern for the gross stability of the structure, these strategies must involve strengthening of either the structure itself or the adjacent geologic materials.

8.3.1. Considerations for circular tunnels

One concern for the life of a tunnel structure is the quality of contact between the liner and the surrounding geologic media. The quality of contact may be investigated by taking core samples or geophysical techniques, and may be improved by contact grouting or other means. In some cases, the tunnel is in such poor condition or so highly distressed that contact grouting will not provide adequate strength improvement. Some means for strengthening these tunnels may include replacing the lining, increasing the lining thickness by adding reinforced concrete, or adding reinforcement with reinforcing bars or an internal steel liner. Increasing lining thickness does not always provide an acceptable solution, because increasing the structural stiffness will tend to attract more force to the lining. Measures to increase ductility (ability to absorb deformation) as well as strength may prove to be more effective (Power et al., 1996).

If excessive axial or bending stresses are predicted, the retrofit solution may be to provide additional ductility, rather than strength, to the lining. Thickening the lining will not effectively reduce the longitudinal axial or bending stresses unless the strains transmitted to the lining are reduced due to increased soil−structure interaction with the thicker lining. Adding circumferential joints along the axis of the tunnel can reduce the stresses and strains in the lining induced by longitudinally propagating waves. The value of adding joints must be weighed against the expected performance of the liner without joints. Often, reinforcement in the lining can provide adequate ductility. If joints are installed, it is important that they do not become weak

spots where local transverse shear deformation may occur. The ability of the joint to prevent water leakage must also be considered (Power, et al., 1996; Hashash et al., 1998). This approach was used in the retrofit design implementation for the Alameda Tubes in the San Francisco Bay Area.

8.3.2. Considerations for cut-and-cover tunnels

If analyses indicate that the cross-section will be unable to resist imposed racking deformations or seismic earth pressures, structural modifications must be considered. Some possible strategies include increasing the ductility of reinforced concrete linings, adding confining reinforcement at existing linings and columns, and adding steel plate jackets at joints. The addition of joints may be considered to increase longitudinal flexibility.

8.4. Design considerations for structural support members

The design methods described in Section 7 provide the magnitude of deformations and forces in the structural support members of underground structures. The following are some of the issues that the designer may consider when developing the detailed designs of the structural members:

1. Earthquake effects on underground structures take the form of deformations that cannot be changed significantly by strengthening the structure. The structure should instead be designed with sufficient ductility to absorb the imposed deformations without losing the capacity to carry static loads. However, providing sufficient ductility is not analogous to eliminating moment resistance in the frame. Cut-and-cover structures with no moment resistance are susceptible to collapse under the dynamic action of the soil backfill (Owen and Scholl, 1981).

2. Curvature distortion: the ground shaking may cause large curvature distortion in tunnel. The structure can be articulated with transverse joints designed to reduce the estimated distortion and reduce straining of the tunnel structure (Kuesel, 1969).

3. Elastic distortion capacity: the elastic racking distortion capacity of a continuous structural frame may be calculated as the rotation capacity of the most rigid exterior corner joint of the cell. If the elastic rotation capacity of the most rigid corner exceeds the imposed shearing distortion, no further provisions are necessary (Kuesel, 1969).

4. Allowable plastic distortion capacity: if the imposed shearing distortion exceeds the elastic rotation capacity of the most rigid corner joint, plastic distortion will be imposed on the less rigid mem-

ber at that joint. The elastic rotation of the other member may be deducted from the imposed soil distortion to determine the maximum end rotation of the plastically deformed member. If the imposed rotation exceeds this value for a single member, the joint may be designed to distribute plastic yielding to both members of the joint, by equalizing their elastic stiffnesses (this will only be necessary in most unusual circumstances) (Kuesel, 1969). Shear failure should be prevented in members experiencing plastic yielding.

5. The buckling strength of a tunnel lining may be considered, especially when the lining is thin. Desai et al. (1997) has undertaken a discussion of some of these concerns.

6. Where rigid diaphragms act together with flexible structural frames, the distortion of the frame may be prevented adjacent to the diaphragm (as at the end wall of a subway station). Special construction joints may be required in the exterior wall, roof and floor slabs adjacent to the diaphragm to absorb this displacement. An alternate would be to increase the reinforcement.

7. In static design, vertical reinforcing steel on the inside face of exterior walls is necessary only in the mid height regions of the walls. However, during seismic racking these walls will experience tension, so the interior reinforcing steel must be extended into the top and bottom slabs.

8. When structural members that have no direct contact with the soil are continuous with stiff outer structural shell elements that are strained beyond their elastic rotation capacity, these internal members may also suffer plastic rotation. In such cases, ductile sections or hinges should be designed into the connections between these elements. Interior columns, walls, beams, and slabs should be designed to resist dynamic forces normal to their longitudinal axes.

9. Compression struts: the design and detailing of axial members in compression should receive special attention at end connections and the effect of racking of the whole structure should also be attended to. Compressive members acting in concert with continuous diaphragms (e.g. floor slabs) usually will require special detailing to ensure their acting in accordance with design assumptions.

10. Appurtenant structures: where the imposed ground shearing distortion does not strain the main structural frame beyond its elastic capacity, all appendages may be treated as rigidly attached (and may be designed as integral parts of the main structure). Where plastic deformation of the main framework is anticipated, major appendages should preferably be designed as loosely attached
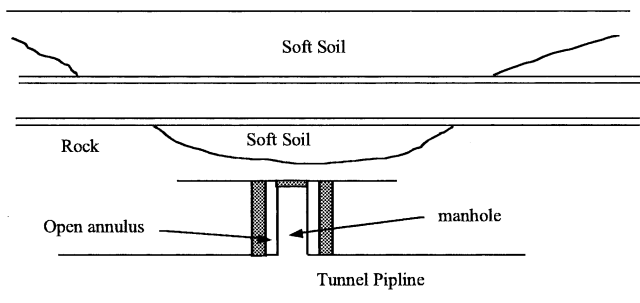
Fig. 25. Tunnel access detail, Los Angeles inland feeder.

(the joint must be designed to be easily repairable or to accommodate differential movement). Local protrusions in such cases may be rigidly attached, with special attention given to detailing the connection to assure ductility. If the connection is detailed to absorb the imposed deformation, local protrusions in such cases may be rigidly attached. For example, the water tunnels for the Los Angeles Inland Feeder project were designed with open space access, Fig. 25, to permit displacements.

11. At the ends of rectangular structures, the joints between the end walls and the roof and sidewall slabs must accommodate differential deformations. The junction of the roof slab to the end wall must accommodate a transverse differential motion equivalent to the imposed shearing displacement between the top and bottom slabs. Intermediate floor slabs must accommodate similar, proportionately smaller displacements. The joint between the sidewall and end wall must accommodate the transverse racking distortion expected for the structure. The deformation joints between end walls and longitudinal side, roof, and floor slabs should preferably be located in the longitudinal slabs. The joints should be accessible to permit repair of overstressed members after an earthquake.

12. The prime consideration in deformation joint location is that no collapse be imminent because of plastic deformation of the structural frame. At all joints where plastic deformation is anticipated or special joints are used, provisions to prevent water leakage must be made. A local reservoir of bentonite, or a rubber gasket can serve this purpose.

8.5. Design strategies for ground failures

Although it is generally not feasible to design the supports for underground structures to resist large permanent ground deformations resulting from failures described in Section 5.1, ground stabilization techniques such as ground improvement, drainage, soil
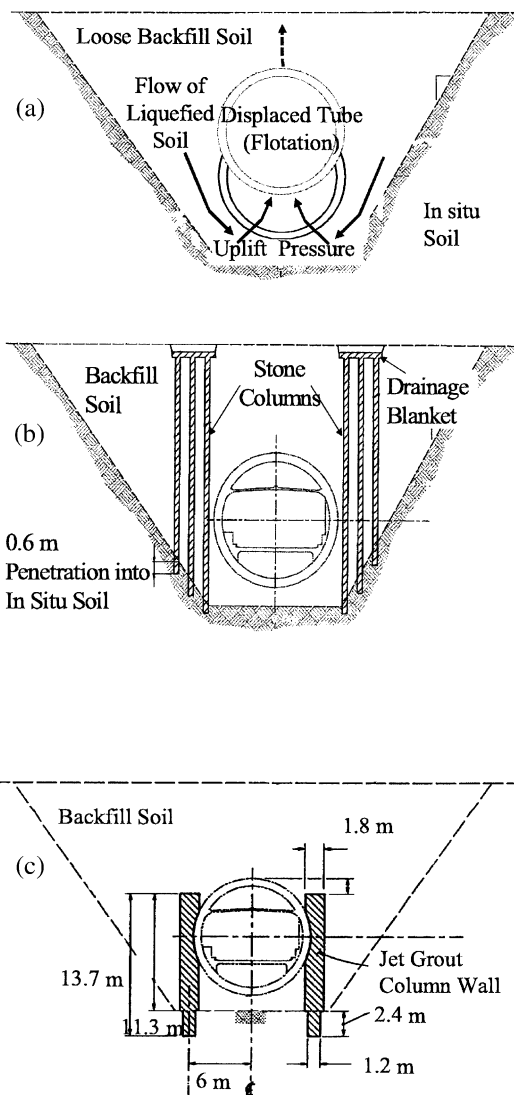

Fig. 26. Isolation principle, use of cut-off walls to prevent tunnel uplift due to liquefaction (after Schmidt & Hashash, 1999). (a) Flotation mechanism. (b) Isolation wall using stone columns, Webster steel tube. (c) Isolation wall using jet grouting for Posey tube.

reinforcement, grouting, or earth retaining systems may be effective in preventing large deformations. Other alternatives include removing problem soils or in the case of a new tunnel, relocating the tunnel alignment. This section provides approaches and guidelines for the design of underground structures to mitigate certain problems associated with ground failure.

8.5.1. Flotation in liquefiable deposits

One of the problems that underground structures can experience in liquefied soil is flotation (Section 5.1.1). Schmidt and Hashash (1999) describe the possible flotation mechanism of a tunnel in a liquefiable layer. As the tunnel experiences uplift the liquefied soil moves underneath the displaced tunnel, further lifting it up. One method to prevent uplift of low-specific

weight underground structures is through the use of cut-off walls and the isolation principle as described in Schmidt and Hashash (1999) and illustrated in Fig. 26. These cutoff walls can be either sheet pile walls or improved soil such as jet grout columns or stone columns (Schmidt et al., 1998). Sheet piles with drain capability (SPDC) can also reduce the excess pore water pressure induced by earthquakes (Kita et al., 1992). Shaking table tests run by Tanaka et al. (1995) showed that SPDC prevented uplift in structures that suffered such damage with ordinary sheet piling.

Barrier walls reduce the rise of excess pore water pressure both on the bottom part of the underground structure and in the ground under it. Uplift with longer barrier walls is smaller than that with shorter walls, showing that the barrier walls effectively reduce the uplift velocity and cumulative vertical displacement of the underground structure models (Ninomiya et al., 1995; Schmidt et al., 1998). It is also more difficult to uplift a wider underground structure.

Once the liquefaction potential is mitigated, the use of flexible joints that allow for differential displacement may still be required for tunnel connections.

8.5.2. Slope instability and lateral spreading

The only technically feasible way to mitigate slope instability (landsliding) or liquefaction-induced lateral spreading movements is to stabilize the ground. It is doubtful that an underground structure can be designed to resist or accommodate these movements unless the hazard is localized and the amount of movement is small (Power et al., 1996).

8.5.3. Underground structures crossing active faults

The general design philosophy is to design the structure to accommodate expected fault displacements, and allow repair of damaged lining afterwards.

One of the methods to estimate the fault displacements is to use empirical relationships that express the expected displacements as function of some source parameters. Using a worldwide database of source parameters for 421 historical earthquakes, empirical relationships among magnitude, rupture length, rupture width, rupture area, and surface displacement have been developed (Wells and Coppersmith, 1994). Maximum and average surface displacements were correlated with both moment magnitude and surface rupture length. Correlation between displacement and moment magnitude appears to be slightly stronger than between displacement and surface rupture length.

A relatively new framework for evaluating fault displacement hazard was presented by Coppersmith and Youngs (2000). The probabilistic fault displacement hazard analysis (PFDHA) is an extension of probabilistic seismic hazard analysis (PSHA), and is composed of the same elements as PSHA. For the assessment of

fault displacement hazard, the predictive relationship for ground motion in step 3 of PSHA (Section 4.2) is replaced with a displacement attenuation function. However, unlike the predictive relationships for ground motion, which are supported by relatively significant amount of empirical data, the models for fault displacement hazard are currently in the initial stages of development. An alternative method related to PSHA called the displacement approach uses the observations at the specified location of interest to assess the hazard (Coppersmith and Youngs, 2000). By evaluating the hazard only with the observed frequency and the amount of displacement events, the displacement approach implicitly considers sources of earthquakes and seismicity. The method reduces the steps normally required for PSHA, but is likely to require region-specific data. Both of these methodologies have been utilized for the assessment of fault displacement hazard at Yucca Mountain, a potential high level nuclear waste repository (Coppersmith and Youngs, 2000).

Design strategies for tunnels crossing active faults depend on the magnitude of displacement and the width of the zone over which that displacement is distributed. If large displacements are concentrated in a narrow zone, retrofit design will most likely consist of enlarging the tunnel across and beyond the displacement zone. This has been discussed in a number of publications, including Rosenbleuth (1977), Owen and Scholl (1981), Brown et al. (1981), Desai et al. (1989), Rowe (1992), and Abramson and Crawley (1995), and has been implemented in the San Francisco BART system and Los Angeles Metro rapid-transit tunnel system. This method provides adequate clearance for repair to roads or rails even when the tunnel is distorted by creeping displacements. The Berkeley Hills Tunnel for the BART system employs concrete-encased steel ribs, which are particularly suitable because they provide sufficient ductility to accommodate distortions with little degradation of strength. Under axial fault displacement, relative slip placing a tunnel in compression tends to be more damaging than slip that would elongate the tunnel. However, the development of cracks in the lining due to both elongation and compression may result in unacceptable water inflow. When watertightness is a necessity, flexible couplings may provide an adequate solution (Wang, 1993). This solution was used for the South West Ocean Outfall in San Francisco. Further discussion of reinforced concrete tubes in fault zones is provided by Hradilek (1977).

The length over which enlargement is made is a function of both the amount of fault displacement and the permissible curvature of the road or track. The longer the enlarged tunnel, the smaller will be the post-earthquake curvature (Power et al., 1996).

An enlarged tunnel may also surround an inner

tunnel that is backfilled with frangible backpacking such as cellular concrete. Cellular concrete has relatively low yield strength to minimize lateral loads on the tunnel liner, but has adequate strength to resist normal soil pressures and other seismic loads such as minor ground shock and soil loosening load or other vertical loads above the excavation. It also has stable long-term properties with respect to age hardening, chemical resistance, and creep behavior (Power et al., 1996).

If fault movements are small (i.e. less than a few inches) and/or distributed over a relatively wide zone, it is possible that the tunnel may be designed to accommodate the fault displacement by providing articulation of the tunnel liner with ductile joints. This allows the tunnel to distort into an S-shape through the fault zone without rupture. The closer the joint spacing, the better the performance of the liner. Design of a lining to accommodate fault displacement becomes more feasible in soft soils where the tunnel lining can more effectively redistribute the displacements. Again, keeping the tunnel watertight is a concern when using joints (Power et al., 1996).

8.6. Seismic design of high level nuclear waste repositories

The methods described in this report can also be used for the analysis of underground openings used in nuclear waste repositories (NWR). The main difference is in the seismic hazard analysis, whereby the design seismic event corresponds to return periods that are compatible with the design life of the facility. Stepp (1996) presents a report that summarizes many of the specific issues related to seismic design of NWR.

9. Research Needs

The material presented in this report describes the current state of knowledge for the design of underground structures. Many issues require further investigation to enhance our understanding of seismic response of underground structures and improve seismic design procedures. Some of these issues include:

1. Instrumentation of tunnels and underground structures to measure their response during ground shaking. These instruments would include measurement of vertical and lateral deformations along the length of the tunnel. This will be useful to understand the effect of spatial incoherency and directivity of the ground motion on tunnel response. Other instrumentation would be useful to measure differential movement between a tunnel

and a portal structure, and to measure racking of rectangular structures such as subway stations.
2. Improved evaluation of the mechanism of the load transferred from the overburden soil to the ceiling slab of a cut and cover structure. Not all of the inertia force of the overburden soil is transferred to the ceiling slab; however, research into the evaluation of the soil block that provides inertia force has not yet been undertaken (Iida et al., 1996).
3. Research into the influence of high vertical accelerations on the generation of large compressive loads in tunnel linings and subway station columns. Large vertical forces may have been a factor in the collapse of the Daikai Subway station (Iida et al., 1996).
4. Development of improved numerical models to simulate the dynamic soil structure interaction problem of tunnels, as well as portal and subway structures. These models will be useful in studying the effect of high velocity pulses generated near fault sources on underground structures (Hashash et al., 1998).
5. Evaluation of the significance of ground motion directivity and 'fling effect' on tunnel response.
6. Evaluation of the significance of ground motion incoherence on the development of differential movement along the length of a tunnel (Power et al., 1996). Ground motion incoherence is particularly important in soft soils and shallow tunnels where the potential for slippage between the tunnel and soil is high.
7. Evaluation of the influence of underground structures on the local amplification or attenuation of propagated ground motion.
8. Research into the effects of repeated cyclic loading on underground tunnels (St. John and Zahrah, 1987).
9. Research into the application of non-conventional lining, bolting, and water insulation materials that can be used for seismic joints and to enhance the seismic performance of the tunnel.

10. In memoriam

Dr Birger Schmidt has been the main motivating force behind the development of this report. Dr Birger Schmidt, a native of Denmark, passed away on October 2, 2000 after a yearlong fight with cancer. He had a distinguished career in geotechnical engineering spanning almost four decades. His many contributions include the error-function method for estimating settlements due to tunneling as well as over 80 technical publications. He actively contributed to the many ef-

forts of the International Tunnelling Association (ITA) Working Group No 2: Research. He maintained his interest and support of this report through the last week of his life and emphasized the need to complete this work.

This report is dedicated to his memory. He has been a friend and a mentor and will be greatly missed.

Youssef Hashash

11. Addendum

The reference of Power et al. (1996) has been updated and will be issued soon as part of a report by the Multidisciplinary Center for Earthquake Engineering Research (MCEER), Buffalo, NY to the U.S. Federal Highway Administration. The update contains many details that are complementary to the material presented in this report and contains revised values for Table 2 based on the work of Sadigh and Egan (1998).

Appendix A: List of symbols

α:	Coefficient used in calculation of lining–soil racking ratio of circular tunnels
α^n:	Coefficient used in calculation of lining–soil racking ratio of circular tunnels under normal loading only
β_1:	Coefficient used in developing loading criteria for ODE
ε^{ab}:	Total axial strain
$\varepsilon^a_{\max}$:	Maximum axial strain caused by a 45° incident shear wave
$\varepsilon^b_{\max}$:	Maximum bending strain caused by a 0 degree incident shear wave
ε_l:	Longitudinal strain
ε_{1m}:	Maximum longitudinal strain
ε_n:	Normal strain
ε_{nm}:	Maximum normal strain
ϕ:	Angle of incidence of wave with respect to tunnel axis
γ_s:	Simple shear strain of a soil element
γ:	Shear strain
γ_m:	Maximum shear strain
$\gamma_{\max}$:	Maximum free-field shear strain of soil or rock medium
γ_t:	Soil unit weight
σ^{ab}:	Total axial stress
θ:	Angular location of the tunnel lining
ρ:	Radius of curvature
ρ_m:	Density of medium
$\rho_{\max}$:	Maximum radius of curvature
τ:	Simple shear stress of a soil element
$\tau_{\max}$:	Maximum shear stress
Δ:	Lateral deflection
$\Delta_{\text{structure}}$:	Racking deflection of rectangular tunnel cross-section
$\Delta d_{\text{free-field}}$:	Free-field diametric deflection in non-perforated ground
Δd_{lining}:	Lining diametric deflection
$\Delta d^n_{\text{lining}}$:	Lining diametric deflection under normal loading only
v_l:	Poisson's ratio of tunnel lining
v_m:	Poisson's ratio of soil or rock medium
Ψ:	Coefficient used in calculation of flexibility ratio of rectangular tunnels
a_1:	Coefficient used in calculation of flexibility ratio of rectangular tunnels
a_2:	Coefficient used in calculation of flexibility ratio of rectangular tunnels
a_P:	Peak particle acceleration associated with P-wave
a_R:	Peak particle acceleration associated with Rayleigh wave
a_{RP}:	Peak particle acceleration associated with Rayleigh Wave for compressional component
a_{RS}:	Peak particle acceleration associated with Rayleigh Wave for shear component
a_S:	Peak particle acceleration associated with S-wave
d:	Diameter or equivalent diameter of tunnel lining
f:	Ultimate friction force between tunnel and surrounding soil
h:	Thickness of the soil deposit
r:	Radius of circular tunnel
t:	Thickness of tunnel lining
A:	Free-field displacement response amplitude of an ideal sinusoidal S-wave
A_a:	Same as A, used for axial strain calculation
A_b:	Same as A, used for bending strain calculation
A_c:	Cross-sectional area of tunnel lining
C:	Compressibility ratio of tunnel lining

C_P: Apparent velocity of P-wave propagation

C_R: Apparent velocity of Rayleigh wave propagation

C_S: Apparent velocity of S-wave propagation

$C_{s(R)}$: Apparent velocity of S-wave propagation in soil due to presence of the underlying rock

$C_{s(s)}$: Apparent velocity of S-wave propagation in soil only

D: Displacement amplitude of soil

D: Effects due to dead loads of structural components

E: Plane strain elastic modulus of frame

$E1$:   Effects due to vertical loads of earth and water

$E2$:   Effects due to horizontal loads of earth and water

E_l: Modulus of elasticity of tunnel lining

E_m: Modulus of elasticity of soil or rock medium

EQ: Effects due to design earthquake motion

EX: Effects of static loads due to excavation

F: Flexibility ratio of tunnel lining

G_m: Shear modulus of soil or rock medium

H: Effects due to hydrostatic water pressure

H: Height of tunnel

I: Moment of inertia of the tunnel lining (per unit width) for circular lining

I_I: Moment of inertia of invert slabs in a rectangular cut-and-cover structure

I_c: Moment of inertia of tunnel lining section

I_R: Moment of inertia of roof slabs in a rectangular cut-and-cover structure

I_W: Moment of inertia of walls in a rectangular cut-and-cover structure

K: Free-field curvature due to body or surface waves

K_m: Free-field maximum curvature due to body or surface waves

K_1:   Full-slip lining response coefficient

K_2:   No-slip lining response coefficient

K_a: Longitudinal spring coefficient of soil or rock medium

K_0:   At rest coefficient of earth pressure

K_t: Transverse spring coefficient of soil or rock medium

L: Effects due to live loads

L: Wavelength of ideal sinusoidal shear wave

L_t: Total length of tunnel

$M(\theta)$: Circumferential bending moment in tunnel lining at angle θ

M_{max}:   Maximum bending moment in tunnel cross-section due to shear waves

P: Concentrated force acting on rectangular structure

Q_{max}:   Maximum axial force in tunnel cross-section due to shear waves

$(Q_{max})_f$: Maximum frictional force between lining and surrounding soils

R: Lining-soil racking ratio

R^n: Lining–soil racking ratio under normal loading only

S_1:   Force required to cause a unit racking deflection of a rectangular frame structure

T: Predominant natural period of a shear wave in the soil deposit

$T(\theta)$: Circumferential thrust force in tunnel lining at angle θ

T_{max}:   Maximum thrust in tunnel lining

U: Required structural strength capacity

$V(\theta)$: Circumferential shear force in tunnel lining at angle θ

V_{max}:   Maximum shear force in tunnel cross-section due to shear waves

V_P: Peak particle velocity associated with P-waves

V_R: Peak particle velocity associated with Rayleigh Wave

V_{RP}:   Peak particle velocity associated with Rayleigh Wave for compressional component

V_{RS}:   Peak particle velocity associated with Rayleigh Wave for shear component

V_S: Peak particle velocity associated with S-waves

W: Width of the structure

Y: Distance from neutral axis of cross-section to extreme fiber of tunnel lining

Appendix B: Sample calculations

Design example 1: a linear tunnel in soft ground (after Wang, 1993)

In this example, a tunnel lined with a cast-in-place circular concrete lining (e.g. a permanent second-pass support), is assumed to be built in a soft soil site. The geotechnical, structural, and earthquake parameters are listed as follows:

Geotechnical Parameters:

- Apparent velocity of S-wave propagation, $C_s = 110$ m/s
- Soil unit weight, $\gamma_t = 17.0$ kN/m³
- Soil Poisson's ratio, $\nu_m = 0.5$ (saturated soft clay)
- Soil deposit thickness over rigid bedrock, $h = 30.0$ m

Structural Parameters:

- Lining thickness, $t = 0.30$ m
- Lining diameter, $d = 6.0$ m → $r = 3.0$ m

- Length of tunnel, $L_t = 125$ m
- Moment of inertia of the tunnel section, I_c
  $= \dfrac{\pi(3.15^4 - 2.85^4)}{4}(0.5) = 12.76$ m^4 (one half of the full section moment of inertia to account for concrete cracking and non-linearity during the MDE)
- Lining cross section area, $A_c = 5.65$ m^2
- Concrete Young's Modulus, $E_l = 24\,840$ MPa
- Concrete yield strength, $f_c = 30$ MPa
- Allowable concrete compression strain under combined axial and bending compression, $\varepsilon_{allow} = 0.003$ (during the MDE)

Tunnel Cross Section
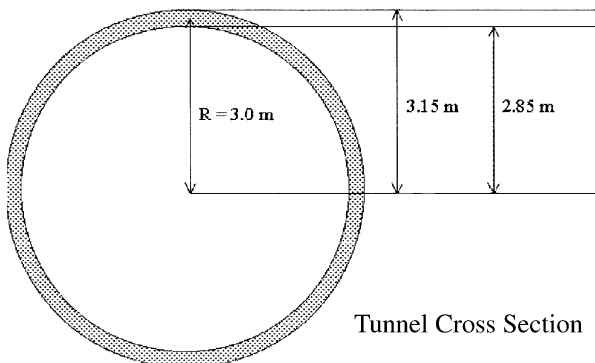
Tunnel Geometry for Example 1

Earthquake parameters (for the MDE):

- Peak ground particle acceleration in soil, $a_s = 0.6$ g
- Peak ground particle velocity in soil, $V_s = 1.0$ m/s

First, try the simplified equation. The angle of incidence (ϕ) of 40° gives the maximum value for longitudinal strain (ε^{ab}), the combined maximum axial strain and curvature strain is calculated as:

$$\varepsilon^{ab} = \pm \frac{V_s}{C_s}\sin\phi\,\cos\phi \pm \frac{a_s r}{C_s^2}\cos^3\phi$$

$$= \pm \frac{1.0}{2(110)}\sin(40°)\cos(40°)$$

$$\pm \frac{(0.6)(9.81)(3.0)}{(110)^2}\cos^3(45°) = \pm 0.0051.$$

Eq. (6)

The calculated maximum compression strain exceeds the allowable compression strain of concrete (i.e. $\varepsilon^{ab} > \varepsilon_{allow} = 0.003$).

Now use the tunnel−ground interaction procedure.

1. Estimate the predominant natural period of the soil deposit (Dobry et al., 1976):

$$T = \frac{4h}{C_s} = \frac{(4)(30.0)}{110} = 1.09 s$$

Eq. (16)

2. Estimate the idealized wavelength:

$$L = TC_s = 4h = 4(30.0) = 120 \text{ m}$$

Eq. (15)

3. Estimate the shear modulus of soil: $G_m = \rho_m C_s^2$
$= \dfrac{17.0}{9.81}(110)^2 = 20\,968$ kPa

4. Derive the equivalent spring coefficients of the soil:

$$K_a = K_t = \frac{16\pi G_m (1 - v_m)}{(3 - 4v_m)}\frac{d}{L}$$

$$= \frac{(16\pi)(20\,968)(1 - 0.5)}{(3 - (4)(0.5))}\left(\frac{6.0}{120}\right)$$

$$= 26\,349 \text{ kN/m}$$

Eq. (14)

5. Derive the ground displacement amplitude, A:

The ground displacement amplitude is generally a function of the wavelength, L. A reasonable estimate of the displacement amplitude must consider the site-specific subsurface conditions as well as the characteristics of the input ground motion. In this design example, however, the ground displacement amplitudes are calculated in such a manner that the ground strains as a result of these displacement amplitudes are comparable to the ground strains used in the calculations based on the simplified free-field equations. The purpose of this assumption is to allow a direct and clear evaluation of the effect of tunnel−ground interaction. Thus, by assuming a sinusoidal wave with a displacement amplitude A and a wavelength L, we can obtain:

For free-field axial strain:

$$\frac{V_s}{C_s} = \frac{2\pi A}{L} = \frac{V_s}{C_s}\sin\phi\,\cos\phi \Rightarrow$$

$$A = \frac{(120)(1.0)}{2\pi(110)}\sin(40°)\cos(40°)$$

$$= 0.085 \text{ m.}$$

Eq. (17)

Let $A_a = A = 0.085$ m.
For free-field bending curvature:

$$\frac{a_s}{C_s^2}\cos^3\phi = \frac{4\pi^2 A}{L^2} \Rightarrow A = \frac{(120^2)(0.6)(9.81)}{4\pi^2(110^2)}$$

$$\cos^3(\phi) = 0.080 \text{ m.}$$

Eq. (18)

Let $A_b = A = 0.080$ m.

6. Calculate the maximum axial strain and the corresponding axial force of the tunnel lining:

$$\varepsilon^a_{\max} = \frac{\left(\dfrac{2\pi}{L}\right)}{2 + \left(\dfrac{E_l A_c}{K_a}\right)\left(\dfrac{2\pi}{L}\right)^2} A_a$$

$$= \frac{\left(\dfrac{2\pi}{120}\right)}{2 + \left(\dfrac{(24,840,000)(5.65)}{26,349}\right)\left(\dfrac{2\pi}{120}\right)^2}(0.085)$$

$$= 0.00027 \qquad\qquad \text{Eq. (10)}$$

The axial force is limited by the maximum frictional force between the lining and the surrounding soils. Estimate the maximum frictional force:

$$Q_{\max} = (Q_{\max})_f = \frac{fL}{4} = E_l A_c \varepsilon^a_{\max}$$

$$= (24\,840\,000)(5.65)(0.00027)$$

$$= 37\,893 \text{ kN} \qquad\qquad \text{Eq. (10)}$$

7. Calculate the maximum bending strain and the corresponding bending moment of the tunnel lining:

$$\varepsilon^b_{\max} = \frac{\left(\dfrac{2\pi}{L}\right)^2 A_b}{1 + \dfrac{E_l I_c}{K_t}\left(\dfrac{2\pi}{L}\right)^4} r$$

$$= \frac{\left(\dfrac{2\pi}{120}\right)^2 (0.080)}{1 + \dfrac{(24,840,000)(12.76)}{26,349}\left(\dfrac{2\pi}{120}\right)^4}(3.0) = 0.00060$$

$$\text{Eq. (11)}$$

$$M_{\max} = \frac{E_l I_c \varepsilon^b_{\max}}{r}$$

$$= \frac{(24,840,000)(12.76)(0.00060)}{3.0}$$

$$= 63\,392 \text{ kN} - \text{m} \qquad\qquad \text{Eq. (12)}$$

8. Compare the combined axial and bending compression strains to the allowable:

$$\varepsilon^{ab} = \varepsilon^a_{\max} + \varepsilon^b_{\max} = 0.00027 + 0.00060$$

$$= 0.00087 < \varepsilon_{allow} = 0.003 \qquad\qquad \text{Eq. (13)}$$

9. Calculate the maximum shear force due to the bending curvature:

$$V_{\max} = M_{\max}\left(\frac{2\pi}{L}\right) = (63,391)\left(\frac{2\pi}{120}\right) = 3319 \text{ kN}$$

$$\text{Eq. (12)}$$

10. Calculate the allowable shear strength of concrete during the MDE:

$$\phi V_c = \frac{0.85\left(\sqrt{f_c'}\,A_{\text{shear}}\right)}{6} = \frac{(0.85)\sqrt{30}}{6}\left(\frac{5.65}{2}\right)(1000)$$

$$= 2192 \text{ kN}$$

where ϕ = shear strength reduction factor (0.85), f_c' = yield strength of concrete (30 MPa), and A_{shear} = effective shear area = $A_c/2$. Note: Using $\phi = 0.85$ for earthquake design may be very conservative.
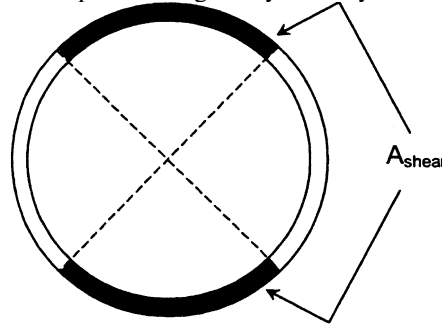
Effective shear area, Example 1

11. Compare the induced maximum shear force with the allowable shear resistance:

$$V_{\max} = 3319 \text{ kN} > \phi V_c = 2192 \text{ kN}$$

Although calculations indicate that the induced maximum shear force exceeds the available shear resistance provided by the plain concrete, this problem may not be of major concern in actual design because:

- The nominal reinforcements generally required for other purposes may provide additional shear resistance during earthquakes.
- The ground displacement amplitudes, A, used in this example are very conservative. Generally, the spatial variations of ground displacements along a horizontal axis are much smaller than those used in this example, provided that there is no abrupt change in subsurface profiles.

Design example 2: axial and curvature deformation due to S-waves, beam-on-elastic foundation analysis method (after Power et al., 1996)

Earthquake and soil parameters:

- $M_w = 6.5$, source-to-site distance = 10 km
- Peak ground particle acceleration at surface, a_{max} = 0.5 g
- Apparent velocity of S-wave propagation in soil due to presence of the underlying rock, $C_{s(R)} = 2$ km/s
- Predominant natural period of shear waves, $T = 2$ s
- Apparent velocity of S-wave propagation in soil only, $C_{s(s)} = 250$ m/s
- Soil density, $\rho_m = 1920$ kg/m^3, stiff soil
- Soil Poisson's ratio, $\nu_m = 0.3$

Tunnel Parameters (Circular Reinforced Concrete Tunnel):

- $d = 6$ m $\rightarrow r = 3.0$ m, $t = 0.3$ m, depth (below ground surface) = 35 m
- $E_l = 24.8 \times 10^6$ kPa, $\nu_l = 0.2$, $A_c = 5.65$ m^2, $I_c = \dfrac{\pi(3.15^4 - 2.85^4)}{4} = 25.4$ m^4 (see tunnel cross section in Appendix B)

1. Determine the longitudinal and transverse soil spring constants:

$$L = C_{s(R)}T = (2000)(2) = 4000 \text{ m},$$
$$G_m = \rho_m C_m^2 = 119\,800 \text{ kPa} \qquad \text{Eq. (15)}$$

$$K_a = K_t = \frac{16\pi G_m(1 - \nu_m)}{(3 - 4\nu_m)} \frac{d}{L}$$

$$= \frac{16\pi(119\,800)(1 - 0.3)}{3 - (4)(0.3)} \frac{6}{4000}$$

$$= 3510 \text{ kPa} \qquad \text{Eq. (14)}$$

2. Determine the maximum axial strain due to S-waves:

Estimate the ground motion at the depth of the tunnel.

$$a_s = 0.7a_{max} = (0.7)(0.5 \ g) = 0.35 \ g \qquad \text{Table 4}$$

$$A = (35 \text{ cm/g})(0.35 \ g) = 12.2 \text{ cm}$$
$$= 0.12 \text{ m} \qquad \text{Table 3}$$

$$\varepsilon_{max}^a = \frac{\left(\dfrac{2\pi}{L}\right)A}{2 + \dfrac{E_l A_c}{K_a}\left(\dfrac{2\pi}{L}\right)^2}$$

$$= \frac{\left(\dfrac{2\pi}{4000}\right)(0.12)}{2 + \dfrac{(24.8)(10^6)(5.65)}{3510}\left(\dfrac{2\pi}{4000}\right)^2}$$

$$= 0.00009 \qquad \text{Eq. (10)}$$

3. Determine the maximum bending strain due to S-waves:

$$\varepsilon_{max}^b = \frac{\left(\dfrac{2\pi}{L}\right)^2 A}{1 + \dfrac{E_l I_c}{k_t}\left(\dfrac{2\pi}{L}\right)^4} r$$

$$= \frac{\left(\dfrac{2\pi}{4000}\right)^2 (0.12)}{1 + \dfrac{(24.8)(10^6)(25.4)}{3510}\left(\dfrac{2\pi}{4000}\right)^4} \qquad (3)$$

$$= 0.0000003 \qquad \text{Eq. (11)}$$

4. Determine combined strain:

$$\varepsilon^{ab} = \varepsilon_{max}^a + \varepsilon_{max}^b = 0.00009 + 0.00000030$$
$$\approx 0.00009 \qquad \text{Eq. (13)}$$

If the calculated stress from the beam-on-elastic foundation solution is larger than from the free-field solution, the stress from the free-field solution should be used in design.

Design example 3: ovaling deformation of a circular tunnel (modified from Power et al., 1996)

Earthquake and soil parameters:

- $M_w = 7.5$, source-to-site distance = 10 km
- Peak ground particle acceleration at surface, a_{max} = 0.5 g
- Stiff soil, $\rho_m = 1920$ kg/m^3, $C_m = 250$ m/s, $\nu_m = 0.3$

Tunnel parameters (circular reinforced concrete tunnel):

- $d = 6$ m $\rightarrow r = 3.0$ m
- $t = 0.3$ m, depth = 15 m (see tunnel cross-section in Appendix B)
- $E_l = 24.8 \times 10^6$ kPa, $\nu_l = 0.2$
- Area of the tunnel lining (per unit width), $A_l = 0.3$ m^2/m
- Moment of inertia of the tunnel lining (per unit width), $I = \dfrac{1}{12}(1)(0.3^3) = 0.0023$ m^4/m

Use formulations of Penzien (2000) assuming full slip condition.

Note: in the following calculation, more significant figures are kept throughout each step to show that formulations of Penzien (2000) give the same values as Wang (1993).

1. Determine the racking ratio (R^n) and the displacement term $\Delta D^n_{\text{lining}}$:

Estimate ground motion at depth of tunnel.

$$a_s = 0.9a_{\max} = (0.9)(0.5 \text{ g}) = 0.45 \text{ g} \qquad \text{Table 4}$$

Assuming stiff soil,

$$V_s = (140 \text{ cm/s/g})(0.45 \text{ g}) = 63 \text{ cm/s}$$
$$= 0.63 \text{ m/s} \qquad \text{Table 2}$$

$$\gamma_{\max} = \frac{V_s}{C_m} = \frac{0.63}{300} = 0.0021$$

$$G_m = \rho_m C_m^2 = \left(\frac{1920}{1000}\right)(250^2) = 120\,000 \text{ kPa} \qquad \text{Table 5}$$

$$E_m = 2G_m(1 + \nu_m) = 2(120\,000)(1 + 0.3)$$
$$= 312\,000 \text{ kPa}$$

$$\alpha^n = \frac{12 E_l I (5 - 6\nu_m)}{d^3 G_m (1 - \nu_l^2)}$$
$$= \frac{(12)(24.8)(10^6)(0.0023)(5 - (6)(0.3))}{(6^3)(120\,000)(1 - (0.2^2))}$$
$$= 0.088025 \qquad \text{Eq. (34)}$$

$$R^n = \frac{4(1 - \nu_m)}{\alpha^n + 1} = \frac{4(1 - 0.3)}{0.088025 + 1} = 2.5735 \qquad \text{Eq. (33)}$$

$$\Delta d^n_{\text{lining}} = R^n \Delta d_{\text{free-field}} = R^n \frac{\gamma_{\max} d}{2}$$
$$= (2.5735)\frac{(0.0021)(6)}{2} = 0.016213 \qquad \text{Eq. (29)}$$

2. Determine the maximum tangential thrust (T) and moment (M) due to S-waves:

$$T\left(\frac{\pi}{4}\right) = \frac{12 E_l I \Delta d^n_{\text{lining}}}{d^3 (1 - \nu_l^2)} \cos^2\left(\theta + \frac{\pi}{4}\right)$$
$$= \frac{(12)(24.8)(10^6)(0.0023)(0.016213)}{(6^3)(1 - (0.2^2))} \qquad \text{Eq. (30)}$$
$$\times \cos 2\left(\frac{\pi}{4} + \frac{\pi}{4}\right) = 53.5 \text{ kN}$$

$$M\left(\frac{\pi}{4}\right) = \frac{6 E_l I \Delta d^n_{\text{lining}}}{d^2 (1 - \nu_l^2)} \cos^2\left(\theta + \frac{\pi}{4}\right)$$
$$= \frac{(6)(24.8)(10^6)(0.0023)(0.016213)}{(6^2)(1 - (0.2^2))} \qquad \text{Eq. (31)}$$
$$\times \cos 2\left(\frac{\pi}{4} + \frac{\pi}{4}\right) = 160.6 \text{ kN} - \text{m}$$

Note: maximum T and M occur at $\theta = \pi/4$.

3. Determine combined stress σ and strain ε from thrust and bending moment:

$$\sigma = \frac{T(\theta)}{A_l} + \frac{M(\theta)Y}{I} = \frac{53.5}{0.3} + \frac{(160.6)(0.15)}{0.0023}$$
$$= 178 + 10474 = 10\,652 \text{ kPa}$$

Use formulations of Wang (1993) assuming full slip condition.

1. Determine the flexibility ratio (F) and full-slip lining response coefficient (K_1):

$$F = \frac{E_m(1 - \nu_l^2)r^3}{6 E_l I (1 + \nu_m)}$$
$$= \frac{(312\,000)(1 - 0.2^2)(3^3)}{6(24.8)(10^6)(0.0023)(1 + 0.3)}$$
$$= 18.1767 \qquad \text{Eq. (20)}$$

$$K_1 = \frac{12(1 - \nu_m)}{2F + 5 - 6\nu_m} = \frac{12(1 - 0.3)}{2(18.1767) + 5 - 6(0.3)}$$
$$= 0.21237 \qquad \text{Eq. (24)}$$

2. Determine the maximum tangential thrust (T) and moment (M) due to S-waves:

$$T_{\max} = \frac{1}{6} K_1 \frac{E_m}{(1 + \nu_m)} r \gamma_{\max}$$
$$= \frac{1}{6}(0.21237)\frac{(312\,000)}{(1 + 0.3)}(3)(0.0021)$$
$$= 53.5 \text{ kN} \qquad \text{Eq. (22)}$$

$$M_{\max} = \frac{1}{6} K_1 \frac{E_m}{(1 + \nu_m)} r^2 \gamma_{\max}$$
$$= \frac{1}{6}(0.21237)\frac{(312\,000)}{(1 + 0.3)}(3^2)(0.0021)$$
$$= 160.6 \text{ kN} - \text{m} \qquad \text{Eq. (23)}$$

3. Determine combined stress σ and strain ε from thrust and bending moment:

$$\sigma = \frac{T}{A_l} + \frac{MY}{I} = \frac{53.5}{0.3} + \frac{(160.6)(0.15)}{0.0023}$$
$$= 178 + 10474 = 10\,652 \text{ kPa}$$

The above calculation is repeated for no-slip condition. The results are summarized in the table below:

	Wang (1993)		Penzien (2000)	
	Full Slip	No Slip	Full Slip	No Slip
T (kN)	53.5	870.9	53.5	106.0
M (kN-m)	160.6	160.6*	160.6	158.9
σ (kPa)	10 652	13 376	10 652	10 716

*Assumed equal to full-slip condition

Note: in the case of full-slip condition, the two formulations give the same values for the force components. It can be observed that magnitude of the moment has a much stronger influence than thrust over the stresses experienced by the tunnel lining. Calculation also shows that under no-slip assumption, the formulation of Wang (1993) yields a much higher thrust than the one from Penzien (2000).

Design example 4: racking deformation of a rectangular tunnel (after Power et al., 1996)

Earthquake and Soil Parameters:

- M_w = 7.5, source-to-site distance = 10 km
- Peak ground particle acceleration at surface, a_{max} = 0.5 g
- Apparent velocity of S-wave propagation in soil, C_m = 180 m/s
- Soft soil, soil density, ρ_m = 1920 kg/m³

Tunnel parameters (rectangular reinforced concrete tunnel):

- Width of tunnel (W) = 10 m, height of tunnel (H) = 4 m, depth to top = 5 m

1. Determine the free-field shear deformation $\Delta_{\text{free-field}}$:
Estimate ground motion at depth of tunnel.

$$a_s = 1.0 a_{max} = (1.0)(0.5\ g) = 0.5\ g \qquad \text{Table 4}$$

Assuming soft soil,

$$V_s = (208\ \text{cm/s/g})(0.5\ g) = 104\ \text{cm/s}$$

$$= 1.0\ \text{m/s} \qquad \text{Table 2}$$

$$\gamma_{max} = \frac{V_s}{C_m} = \frac{1.0}{180} = 0.0056 \qquad \text{Table 5}$$

$$\Delta_{\text{free-field}} = \gamma_{max} H = (0.0056)(4) = 0.022\ \text{m} \qquad \text{Eq. (43)}$$

2. Determine the flexibility ratio F:

$$G_m = \rho_m C_m^2 = \left(\frac{1920}{1000}\right)(180^2) = 62\,000\ \text{kPa} \qquad \text{Table 5}$$

$$F = \frac{G_m W}{S_1 H} \qquad \text{Eq. (45)}$$

Through structural analysis, the force required to cause a unit racking deflection (1 m) for a unit length (1 m) of the cross-section was determined to be 310 000 kPa. Note that for the flexibility ratio F to be dimensionless, the units of S must be in force per area.

$$F = \frac{(62000)(10)}{(310\,000)(4)} = 0.5$$

For F = 0.5, the racking coefficient R is equal to 0.5.

3. Determine the racking deformation of the structure $\Delta_{\text{structure}}$:

$$\Delta_{\text{structure}} = R\Delta_{\text{free-field}} = (0.5)(0.022) = 0.011\ \text{m} \qquad \text{Eq. (51)}$$

Determine the stresses in the liner by performing a structural analysis with an applied racking deformation of 0.011 m. Both the point load and triangularly distributed load pseudo-lateral force models should be applied to identify the maximum forces in each location of the liner.

References

American Association of State Highway and Transport Officials (AASHTO), 1991. Standard Specifications for Highway Bridges.

ACI 318, 1999. Building Code Requirements for Reinforced Concrete, American Concrete Institute

Abramson, L.W., Crawley, J.E., 1995. High-speed rail tunnels in California. Proceedings of the 1995 Rapid Excavation and Tunneling Conference, June 18–21, San Francisco, CA, USA.

Abrahamson, N.A., 1985. Estimation of seismic wave coherency, and rupture velocity using the SMART-1 strong motion array recordings. Report no. EERC/UCB/8502, Earthquake Engineering Research Center.

Abrahamson, N.A., 1992. Spatial variation of earthquake ground motion for application to soil-structure interaction. Report no. TR-100463, Electric Power Research Institute.

Abrahamson, N.A., 1995. Review of apparent seismic wave velocities from spatial arrays. Report, Geomatrix Consultants, San Francisco, CA, USA.

ASCE, 1974. Earthquake damage evaluation and design considerations for underground structures, February. American Society of Civil Engineers, Los Angeles Section.

Bardet, J.P., 1991. LINOS — a Non-linear Finite Element Program for Geomechanics and Geotechnical Engineering, User's Manual. University of Southern California, Los Angeles, CA.

Bechtel/Parsons Brinckerhoff, 1992. Seismic design criteria for underground structures. Appendix B, Section V of Central Artery/Tunnel Project Design Criteria, Massachusetts Highway Department.

Bickel, J.O., Tanner, D.N., 1982. Sunken tube tunnels. In: Bickel, J.O., Keusel, T.R. (Eds.), Tunnel Engineering Handbook, chapter 13. Van Nostrand Reinhold, New York, pp. 354−394.

Borja, R.I., Chao, H-Y, Montans, F.J., Lin, C-H., 1999. Non-linear ground response at Lotung LSST site. J. Geotech. Geoenviron. Eng. 125 (3), 187−197.

BRGM, 1998. CyberQuake V. 1.1, User Guide, Orleans, France.

Brown, I., Brekke, T., Korbin, G., (1981). Behavior of the Bay Area Rapid Transit tunnels through the Hayward fault. UMTA Report no. CA-06-0120-81-1, USDOT.

Burns, J.Q., Richard, R.M., 1964. Attenuation of stresses for buried cylinders. Proceedings of the Symposium on Soil−Structure Interaction, University of Arizona at Tempe, Arizona.

Chang, C.Y., Power, M.S., Idriss, I.M., Somerville, P.G., Silva, W., Chen, P.C., 1986. Engineering characterization of ground motion — task II: observational data on spatial variations of earthquake ground motion. Report no. NUREG/CR-3805, US Nuclear Regulatory Commission, vol. 3.

Code of Federal Regulations, 1978. Appendix A, seismic and geologic siting criteria for nuclear power plants. Title 10, Energy; Part 100 (10 CFR 100), Reactor Site Criteria. Nuclear Regulatory Commission, Washington, DC.

Coppersmith, K.J., Youngs, R.R., 2000. Data needs for probabilistic fault displacement hazard analysis. J. Geodyn. 29, 329−343.

Desai, D.B., Chu, C.-T., Redd, R.E., 1997. Impervious tunnel linings in a land of shakes. Proceedings of the 1997 Rapid Excavation Tunneling Conference, pp. 45−55.

Desai, D.B., Merritt, J.L., Chang, B., 1989. Shake and slip to survive — tunnel design. Proceedings of the 1989 Rapid Excavation and Tunneling Conference, June 11−14, Los Angeles, CA, USA.

Dobry, R., Oweis, I., Urzua, A., 1976. Simplified procedures for estimating the fundamental period of a soil profile. Bull. Seismol. Soc. Am. 66, 4. pp. 1293−1321.

Douglas, W.S., Warshaw, R., 1971. Design of seismic joint for San Francisco Bay Tunnel. J. Struct. Eng. Div., ASCE 97 (ST4), 1129−1141.

Dowding, C.H., Rozen, A., 1978. Damage to rock tunnels from earthquake shaking. J. Geotech. Eng. Div., ASCE 104 (GT2), 175−191.

Duke, C.M., Leeds, D.J., 1959. Effects of Earthquakes on Tunnels: Paper Presented at the RAND Second Protective Construction Symposium, March 24−26.

Earthquake Engineering Research Institute (EERI), (1990). Loma Prieta Earthquake Reconnaissance Report. Earthquake Spectra, EERI, Supplement to vol. 6.

Earthquake Engineering Research Institute (EERI), (1995). Northridge Earthquake Reconnaissance Report, vol.s 1 and 2. Earthquake Spectra, EERI, Supplement C to vol. 11.

EQE International, 1995. The January 17, 1995 Kobe Earthquake: an EQE Summary Report.

Finn, W.D.L., Lee, K.W., Martin, G.R., 1977. An effective stress model for liquefaction. J. Geotech. Eng. Div., ASCE 103 (GT6), 517−533.

Gomez-Masso, A., Attalla, I., 1984. Finite element vs. simplified methods in the seismic analysis of underground structures. Earthquake Eng. Struct. Dyn. 12, 347−367.

Hashash, Y.M.A., Park, D., 2001. Non-linear one-dimensional seismic ground motion propagation in the Mississippi Embayment. Eng. Geol. 62 (1−3), 185−206.

Hashash, Y.M.A., Tseng, W.S., Krimotat, A., 1998. Seismic soil-structure interaction analysis for immersed tube tunnels retrofit. Geotech. Earthquake Eng. Soil Mech. III 2, 1380−1391. ASCE Geotechnical Special Publication no. 75.

Hetenyi, M., 1976. Beams on Elastic Foundation. University of Michigan Press, Ann Arbor, Michigan.

Hibbitt, Karlsson and Sorensen Inc., ABAQUS User's Manual.

Hoeg, K., 1968. Stresses against underground structural cylinders. J. Soil Mech. Found. Div., ASCE 94 (SM4) 833−858.

Hradilek, P.J., 1977. Behavior of underground box conduit in the San Fernando earthquake. The Current State of Knowledge of Lifeline Earthquake Engineering. ASCE, New York, pp. 308−319.

Hwang, R.N., Lysmer, J., 1981. Response of buried structures to traveling waves. J. Geotech. Eng. Div., ASCE 107 (GT2), 183−200.

Idriss, I.M., Seed, H.B., 1968. Seismic response of horizontal soil layers. J. Soil Mech. Found. Div., ASCE 94 (SM4), 1003−1031.

Iida, H., Hiroto, T., Yoshida, N., Iwafuji, M., 1996. Damage to Daikai subway station. Soils and Foundations, Special Issue on Geotechnical Aspects of the January 17 1995 Hyogoken-Nambu Earthquake. Japanese Geotechnical Society, pp. 283−300.

Itasca Consulting Group Inc., 1992. Universal Distinct Element Code (UDEC) — User's Manual.

Itasca Consulting Group Inc., 1995. FLAC^{3D}, Version 3.3: Fast Legrangian Analysis of Continua.

Iwasaki, T., 1984. Earthquake-resistant design of underground pipelines in Japan. Proceedings of the US−Japan Workshop on Seismic Behavior of Buried Pipelines and Telecommunications Systems, December 1984, Tsukaba Science City, Japan, pp. 164−190.

JSCE, 1988. Earthquake Resistant Design for Civil Engineering Structures in Japan. Japanese Society of Civil Engineers, Tokyo.

Japanese Society of Civil Engineers, 1975. Specifications for Earthquake Resistant Design of Submerged Tunnels.

Kaneshiro, J.Y., Power, M., Rosidi, D., 2000. Empirical correlations of tunnel performance during earthquakes and aseismic aspects of tunnel design. Proceedings of the Conference on Lessons Learned From Recent Earthquakes — On Earthquakes in Turkey 1999, November 8−11.

Kawashima, K., 1999. Seismic design of underground structures in soft ground, a review. Proceedings of the International Symposium on Tunneling in Difficult Ground Conditions. Tokyo, Japan.

Kita, H., Iida, T., Nishitani, M., 1992. Experimental study on countermeasures for liquefaction by steel sheet pile with drain. Proceedings of the Tenth World Conference on Earthquake Engineering. pp. 1701−1706.

Kiyomiya, O., 1995. Earthquake-resistant design features of immersed tunnels in Japan. Tunneling Underground Space Technol. 10 (4), 463−475.

Kramer, S., 1996. Geotechnical Earthquake Engineering. Prentice-Hall, Upper Saddle River, NJ, USA.

Kuesel, T.R., 1969. Earthquake Design Criteria for Subways. J. Struct. Div., ASCE ST6, 1213−1231.

Kuribayashi, E., Iwasaki, T., Kawashima, K., 1974. Dynamic behaviour of a subsurface tubular structure. Proceedings of the Fifth Symposium on Earthquake Engineering. India.

Lysmer, J., Ostadan, F., Tabatabaie, M., Tajirian, F., Vahdani, S., 1991. SASSI: A System for Analysis of Soil−structure Interaction — User's Manual. Geotechnical Engineering Division, Civil Engineering Department, University of California at Berkeley, and Bechtel Corporation, San Francisco, California.

Lysmer, J., Udaka, T., Tsai, C.F., Seed, H.B., 1975. FLUSH: A computer program for approximate 3-D analysis of soil−structure interaction problems. Report no. EERC 75−30. Earthquake Engineering Research Center.

Manoogian, M.E., 1998. Surface motion above an arbitrarily shaped tunnel due to elastic SH waves. Geotechnical Earthquake Engineering and Soil Dynamics III. ASCE, Seattle, pp. 754−765. Geotechnical Special Publication no. 75.

Matasovic, N., Vucetic, M., 1995. Seismic response of soil deposits composed of fully saturated clay and sand layers. Proceedings of the First International Conference on Earthquake Geotechnical Engineering, JGS, vol. 1. Tokyo, Japan, pp. 611−616.

Matsubara, K., Hirasawa, K., Urano, K., 1995. On the wavelength for seismic design of underground pipeline structures. Proceedings of the First International Conference on Earthquake Geotechnical Engineering. pp. 587–590.

Matsuda, T., Samata, S., Iwatate, T., 1996. Seismic response analysis for a collapsed underground subway structure with intermediate columns. The 1995 Hyogoken-Nambu Earthquake: Investigation into Damage to Civil Engineering Structures. Japan Society of Civil Engineers Committee of Earthquake Engineering, pp. 277–285.

Menkiti, C., 2001. Personal Communications.

Merritt, J.L., Monsees, J.E., Hendron, A.J., Jr., 1985. Seismic design of underground structures. Proceedings of the 1985 Rapid Excavation Tunneling Conference, vol. 1, pp. 104–131.

Monsees, J.E., Merritt, J.L., 1988. Seismic modelling and design of underground structures. Numerical Methods in Geomechanics. Innsbruck, pp. 1833–1842.

Monsees, J.E., Merritt, J.L., 1991. Earthquake considerations in design of the Los Angeles Metro. Proceedings of the ASCE Conference on Lifeline Earthquake Engineering.

Nakamura, S., Yoshida, N., Iwatate, T., 1996. Damage to Daikai Subway Station During the 1995 Hyogoken-Nambu Earthquake and Its Investigation. Japan Society of Civil Engineers, Committee of Earthquake Engineering, pp. 287–295.

Navarro, C., 1992. Effect of adjoining structures on seismic response of tunnels. Int. J. Numer. Anal. Methods Geomech. 16, 797–814.

NCEER, 1995. Response to the Hyogoken Nambu Earthquake, January 17, 1995.

Newmark, N.M., 1968. Problems in wave propagation in soil and rock. Proceedings of the International Symposium on Wave Propagation and Dynamic Properties of Earth Materials.

Ninomiya, Y., Hagiwara, R., Azuma, T., 1995. Rise of excess pore water pressure and uplift of underground structures due to liquefaction. Proceedings of the First International Conference on Earthquake Geotechnical Engineering. pp. 1023–1028.

Nuttli, O.W., 1979. The relation of sustained maximum ground acceleration and velocity to earthquake intensity and magnitude. Miscellaneous Paper no. S-73-1, Report 16. US Army Corps of Engineers Waterways Experiment Station, Vicksburg, Mississippi.

Okamoto, S., Tamura, C., Kato, K., Hamada, M., 1973. Behaviors of submerged tunnels during earthquakes. Proceedings of the Fifth World Conference on Earthquake Engineering, vol. 1. Rome, Italy, pp. 544–553.

O'Rourke, T.D., 1984. Guidelines for Tunnel Lining Design. ASCE Technical Committee on tunnel lining design of the Underground Technology Research Council.

O'Rourke, T.D., Goh, S.H., Menkiti, C.O., Mair, R.J., 2001. Highway tunnel performance during the 1999 Duzce earthquake. Proceedings of the Fifteenth International Conference on Soil Mechanics and Geotechnical Engineering, August 27–31, 2000. Istanbul, Turkey.

Oughourlian, C.V., Powell, G.H., 1982. ANSR-III: general purpose computer program for non- linear structural analysis. Report no. UCB/EERC 82/21. Earthquake Engineering Research Center.

Owen, G.N., Scholl, R.E., 1981. Earthquake engineering of large underground structures. Report no. FHWA/RD-80/195. Federal Highway Administration and National Science Foundation.

PB, 1991. Trans-Bay Tube Seismic Joints Post-Earthquake Evaluation. Parsons, Brinckerhoff, Quade and Douglas Inc. Report prepared for the Bay Area Rapid Transit District.

Peck, R.B., Hendron, A.J., Mohraz, B., 1972. State of the art in soft ground tunneling. Proceedings of the Rapid Excavation and Tunneling Conference. American Institute of Mining, Metallurgical and Petroleum Engineers, New York, pp. 259–286.

Penzien, J., Wu, C., 1998. Stresses in linings of bored tunnels. Int. J. Earthquake Eng. Struct. Dyn. 27, 283–300.

Penzien, J., 2000. Seismically -induced racking of tunnel linings. Int. J. Earthquake Eng. Struct. Dyn. 29, 683–691.

Power, M.S., Rosidi, D., Kaneshiro, J., 1996. Vol. III Strawman: screening, evaluation, and retrofit design of tunnels. Report Draft. National Center for Earthquake Engineering Research, Buffalo, New York.

Power, M., Rosidi, D., Kaneshiro, J., 1998. Seismic vulnerability of tunnels-revisited. In: Ozedimir, L., (Ed.). Proceedings of the North American Tunneling Conference. Elsevier, Long Beach, CA, USA.

Reiter, L., 1990. Earthquake Hazard Analysis — Issues and Insights. Columbia University Press, New York.

Rosenbleuth, E., 1977. Soil and rock mechanics in earthquake engineering. Proceedings of the International Conference on Dynamic Methods in Soil and Rock Mechanics.

Rowe, R., 1992. Tunneling in seismic zones. Tunnels and Tunneling, 24, 41–44.

Sadigh, R.K., Egan J.A., 1998. Updated relationships for horizontal peak ground velocity and peak ground displacements for shallow crustal earthquakes. Proceedings of the 6th U.S. National Conference on Earthquake Engineering, May 31–June 4, Seattle, WA, USA.

Sakurai, A., Takahashi, T., 1969. Dynamic stresses of underground pipeline during earthquakes. Proceedings of the Fourth World Conference on Earthquake Engineering.

Schmidt, B., Hashash, Y.M.A., 1998. Seismic rehabilitation of two immersed tube tunnels. Proceedings of the World Tunnel Congress '98, Tunnels and Metropolises. pp. 581–586.

Schmidt, B., Hashash, Y., Stimac, T., 1998. US immersed tube retrofit. Tunnels Tunneling Int. 30 (11), 22–24.

Schmidt, B.S., Hashash, Y.M.A., 1999. Preventing tunnel flotation due to liquefaction. Proceedings of the Second International Conference on Earthquake Geotechnical Engineering, June 21–25. Lisboa, Portugal, pp. 509–512.

Schnabel, P.B., Lysmer, J., Seed, B.H. 1972. SHAKE — a computer program for earthquake response analysis of horizontally layered sites. Report no. EERC 72–12. University of California, Berkeley, CA, USA.

Schwartz, C.W., Einstein, H.H., 1980. Improved design of tunnel supports: vol. 1 — simplified analysis for ground–structure interaction in tunneling. Report no. UMTA-MA-06-0100-80-4. US DOT, Urban Mass Transportation Administration.

Seed, H.B., Whitman, R.V., 1970. Design of earth retaining structures for dynamic loads. Proceedings of the ASCE Specialty Conference on Lateral Stresses in the Ground and Design of Earth Retaining Structures.

SFBART, 1960. Technical Supplement to the Engineering Report for Trans-Bay Tube July.

Sharma, S., Judd, W.R., 1991. Underground opening damage from earthquakes. Eng. Geol. 30, 263–276.

Shi, G.H., 1989. Discontinuous deformation analysis — a new numerical model for the static and dynamics of block systems. Ph.D. Thesis. University of California, Berkeley, CA, USA.

St. John, C.M., Zahrah, T.F., 1987. Aseismic design of underground structures. Tunneling Underground Space Technol. 2 (2), 165–197.

Stepp, J.C., 1996. Seismic and dynamic analysis and design considerations for high level nuclear waste repositories. In: Stepp, J.C. (Ed.), A Report by the Subcommittee on Dynamic Analysis and Design of High Level Nuclear Water Repositories. Structural Engineering Institute, ASCE.

Stevens, P.R., 1977. A review of the effects of earthquakes on underground mines. United States Geological Survey Open File Report 77–313. US Energy Research and Development Administration, Reston, VA.

Sweet, J., 1997. Los Angeles Metro Red Line project: seismic analysis of the Little Tokyo Subway Station. Report no. CAI-097-100. Engineering Management Consultants.

Taipei Metropolitan Area Rapid Transit Systems (TARTS) (1989). Railway Tunnel Investigation — Sungshan Extension Project. ATC Inc.

Takada, S., Abdel-Aziz, M., 1997. A new finite element inelastic model for seismic response analysis of the transverse direction of shield tunnels utilizing the seismic deformation method. Proceedings of the Seventh International Conference on Computing in Civil and Building Engineering, August, vol. 3. Seoul, pp. 1893−1898.

Tanaka, H., Kita, H., Iida, T., Saimura, Y., 1995. Countermeasure against liquefaction for buried structures using sheet pile with drain capability. Proceedings of the First International Conference on Earthquake Geotechnical Engineering. pp. 999−1004.

Tohda, J., 1996. Photographs of pipeline damage in Kobe. Soils and Foundations, Special Issue on Geotechnical Aspects of the January 17 1995 Hyogoken-Nambu Earthquake. Japanese Geotechnical Society.

Ueng, T.S., Lin, M.L., Chen, M.H., 2001. Some geotechnical aspects of 1999 Chi-Chi, Taiwan earthquake. Proceedings of the Fourth International Conference on Recent Advances in Geotechnical Earthquake Engineering and Soil Dynamics. SPL-10.1, 5 p.

Wang, J.-N., 1993. Seismic Design of Tunnels: A State-of-the-Art Approach, Monograph, monograph 7. Parsons, Brinckerhoff, Quade and Douglas Inc, New York.

Wells, D.L., Coppersmith, K.J., 1994. New empirical relationships among magnitude, rupture length, rupture width, rupture area, and surface displacement. Bull. Seismol. Soc. Am. 84 (4), 974−1002.

Whitman, R.V., 1990. Seismic design and behavior of gravity retaining walls. Design and Performance of Earth Retaining Structures. Cornell University, pp. 817−842. ASCE Geotechnical Special Publication 25.

Yeh, G.C.K., 1974. Seismic analysis of slender buried beams. Bull. Seismol. Soc. Am. 64, 5. pp. 1551−1562.